Engineering Applications of Artificial Intelligence 90 (2020) 103541

Contents lists available at ScienceDirect

Engineering Applications of Artificial Intelligence

journal homepage: www.elsevier.com/locate/engappai

# Tunicate Swarm Algorithm: A new bio-inspired based metaheuristic paradigm for global optimization ☆

Satnam Kaur [a], Lalit K. Awasthi [a], A.L. Sangal [a], Gaurav Dhiman [b,*]

[a] Department of Computer Science and Engineering, Dr. B. R. Ambedkar National Institute of Technology, Jalandhar 144011, Punjab, India
[b] Department of Computer Science, Government Bikram College of Commerce, Patiala 147001, Punjab, India

ARTICLE INFO

*Keywords:*
Metaheuristics
Constrained optimization
Unconstrained optimization
Engineering design problems
Swarm intelligence

ABSTRACT

This paper introduces a bio-inspired metaheuristic optimization algorithm named Tunicate Swarm Algorithm (TSA). The proposed algorithm imitates jet propulsion and swarm behaviors of tunicates during the navigation and foraging process. The performance of TSA is evaluated on seventy-four benchmark test problems employing sensitivity, convergence and scalability analysis along with ANOVA test. The efficacy of this algorithm is further compared with several well-regarded metaheuristic approaches based on the generated optimal solutions. In addition, we also executed the proposed algorithm on six constrained and one unconstrained engineering design problems to further verify its robustness. The simulation results demonstrate that TSA generates better optimal solutions in comparison to other competitive algorithms and is capable of solving real case studies having unknown search spaces.
Note that the source codes of the proposed TSA algorithm are available at http://dhimangaurav.com/

## 1. Introduction

To minimize or maximize a function in terms of decision variables, optimization approach plays a significant role. Many real-life problems have a large number of solution spaces, which consists of non-linear constraints. Such problems also have high computational cost along with non-convex and complicated in nature (Singh and Dhiman, 2018a; Dhiman and Kumar, 2018c; Singh and Dhiman, 2018b; Dhiman and Kaur, 2018; Singh et al., 2018b; Dhiman and Kumar, 2018a; Kaur et al., 2018; Singh et al., 2018a). Hence, for solving such problems in terms of large number of variables and constraints are very complicated tasks. Further, local optimum solutions as obtained from various classical approaches do not guarantee for the best solution. To resolve these issues, numerous metaheuristic optimization algorithms are proposed by the researchers (Dhiman et al., 2018; Dhiman and Kumar, 2019b; Dhiman and Kaur, 2019b; Dhiman and Kumar, 2019a; Dhiman et al., 2019; Dhiman, 2019c), which are found to be very efficient for solving very complex problems. However, researchers have given more emphasize in developing of metaheuristic algorithms that are computationally inexpensive, flexible, and simple by nature.

In literature, two broad categories of metaheuristics algorithms are discussed, as *single solution based algorithm (SSBA)* and *population based algorithm (PBA)* (Dhiman and Kumar, 2017). In SSBA, a solution is randomly generated and improved until the optimal solution is obtained; whereas in case of PBA, solutions are randomly evolved in a given search space and try to improve until the optimal solution is obtained. However, most of the SSBAs are unable to reach at the level of global optimum solution due the reason of generating random solution. On the other hand, PBAs are able to find the global optimum. Due to this reason, researchers have attracted towards the PBAs nowadays (Singh et al., 2019; Dhiman, 2019a,b; Dehghani et al., 2019; Chandrawat et al., 2017; Singh and Dhiman, 2017; Dhiman and Kaur, 2017; Verma et al., 2018; Kaur and Dhiman, 2019; Dhiman and Kaur, 2019a; Dhiman and Kumar, 2019c; Garg and Dhiman, 2020).

Further PBAs are categorized, based on the theory of evolutionary algorithms (EAs), as logical behavior of physics algorithms, swarm intelligence of particles, and biological behavior of bio-inspired algorithms. Various EAs are motivated by natural processes, which include reproduction, mutation, recombination, and selection. The survival fitness of candidate in a population (i.e., a set of solutions) is the main basis of all these EAs. Algorithms that are based on the law of physics include the various rules of physics, such as electromagnetic force, gravitational force, heating and cooling of materials, and force of inertia. Algorithms that are biologically inspired mostly mimics the intelligence of swarms. Such kind of intelligence can be adopted among colonies of flocks, ants, and so on. Swarm intelligence based algorithms are very popular among the researchers due to its ease

☆ No author associated with this paper has disclosed any potential or pertinent conflicts which may be perceived to have impending conflict with this work. For full disclosure statements refer to https://doi.org/10.1016/j.engappai.2020.103541.

* Corresponding author.
*E-mail address:* gdhiman0001@gmail.com (G. Dhiman).

https://doi.org/10.1016/j.engappai.2020.103541
Received 19 December 2018; Received in revised form 18 November 2019; Accepted 5 February 2020
Available online 17 February 2020

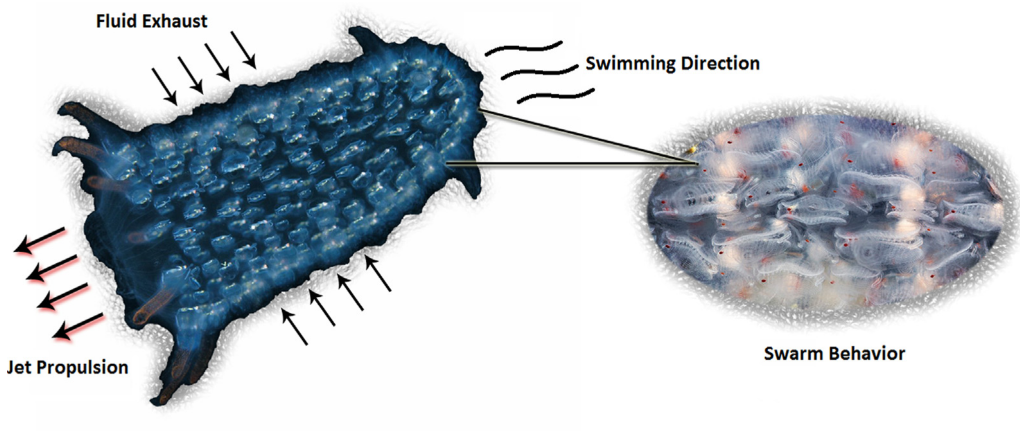


**Fig. 1.** Swarm behavior of tunicate in deep ocean.

of implementation. Its also requires very less number of parameters to be adjusted. Among this category of algorithms, Particle Swarm Optimization (PSO) (Kennedy and Eberhart, 1995) and Ant Colony Optimization (ACO) (Dorigo et al., 2006) are very well-known techniques for the global optimization problems. These kind of algorithms generally mimics the social behavior of fish schooling or bird flocking, where it is assumed that each particle moves around the search space and continuous update its current position *w.r.t.* the global position until satisfactory solution is found.

Optimization algorithms always requires to focus on *exploration* and *exploitation* of a search space (Alba and Dorronsoro, 2005) by maintaining good balancing between them. The exploration process in an algorithm investigates the various promising regions in a search space; whereas exploitation process searches the best solutions over the promising regions (Lozano and Garcia-Martinez, 2010). Hence, to achieve the optimal solutions or near to optimal solutions, these two processes are required to be tuned enough. Having availability of large number of such optimization algorithms, there is always a question raise for the requirement of development of more optimization algorithms. Its answer lies in *No Free Lunch (NFL)* theorem (Wolpert and Macready, 1997), which suggests that a specific optimization algorithm does not solve every problem, because every problem has its own complexity and nature. The *NFL* theorem inspires the researchers to design some new optimization algorithms, which can solve various domain of specific problems.

In this study, authors introduce a novel bio-inspired metaheuristic algorithm, named as Tunicate Swarm Algorithm (TSA), is proposed for optimizing non-linear constrained problems. It is inspired by the swarm behavior of tunicate to survive successfully in the depth of ocean. The main contributions of this work are as follows:

- A bio-inspired tunicate swarm algorithm (TSA) is proposed. The jet propulsion and swarm behaviors of tunicates are examined and mathematically modeled.
- The proposed TSA is implemented and tested on 74 benchmark test functions (i.e., classical, CEC-2015, and CEC-2017).
- The performance of the proposed TSA algorithm is compared with state-of-the-art metaheuristics.
- The efficiency of TSA algorithm is examined for solving the engineering design problems.

The rest of this paper is organized as follows: Section 2 presents the main inspiration and justification of the proposed algorithm. The proposed TSA algorithm is described in Section 3. The experimentation and simulations are presented in Section 4. Section 5 describes the applications of TSA on real-life engineering problems. Finally, the conclusion and future work is given in Section 6.

## 2. Inspiration

Tunicates are bright bio-luminescent, producing a pale blue–green light that can be seen more than many metres away. Tunicates are cylindrical-shaped which are open at one end and closed at the other (Berrill, 1950). Each tunicate is a few millimeters in size. There is a common gelatinous tunic in each tunicate which is helpful to join all of the individuals. However, each tunicate individually draws water from the surrounding sea and producing jet propulsion by its open end through atrial siphons. Tunicate is only animal to move around the ocean with such fluid jet like propulsion. This propulsion is powerful to migrate the tunicates vertically in ocean. Tunicates are often found at depth of 500–800 m and migrate upwards in the upper layer of surface water at night. The size of a tunicate varies from a few centimeter to more than 4 m (Davenport and Balazs, 1991). The most interesting fact of tunicate is their jet propulsion and swarm behaviors (see Fig. 1), which is the main motivation behind this paper.

### 2.1. Motivation

From past few decades, nature-inspired algorithms have gained significant attention from both industry as well as academia. Consequently, numerous algorithms have been provided by researchers after taking inspiration from the nature. In the catalogue of proposed nature-inspired approaches, a majority of algorithms are biology or bio-inspired as they are based on the notion of some characteristics of biological system. Among bio-inspired algorithms, a special class of algorithms have been developed by drawing inspiration from swarm intelligence. Population or Multiple-solution based swarm intelligence algorithms exhibit capability towards solving many real-world optimization problems due to their ability of thoroughly exploring the search space and returning the global optima. However, these approaches cannot solve all optimization problems as also stated by No Free Lunch theorem (Wolpert and Macready, 1997). This fact has motivated us to propose a new population based metaheuristic algorithm with the hope to solve several problems which are hard to solve with existing optimization techniques.

## 3. Tunicate swarm algorithm (TSA)

In this section, the inspiration and mathematical modeling of the proposed algorithm are described in detail.

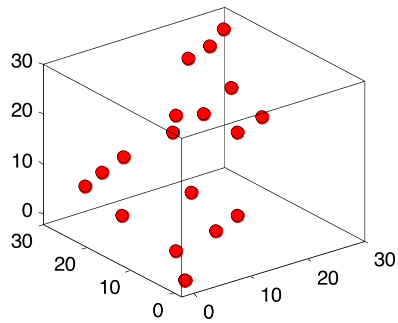


**Fig. 2.** Conflict avoidance between search agents.

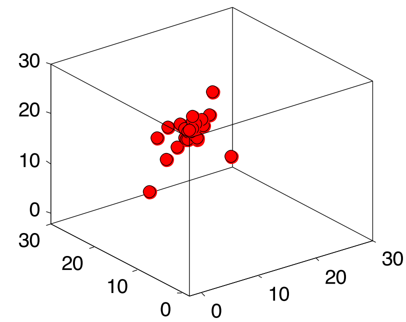


**Fig. 3.** Movement of search agents towards the best neighbor.

### 3.1. Mathematical model and optimization algorithm

Tunicate has an ability to find the location of food source in sea. However, there is no idea about the food source in the given search space. In this paper, two behaviors of tunicate are employed for finding the food source, i.e., optimum. These behaviors are jet propulsion and swarm intelligence.

To mathematically model the jet propulsion behavior, a tunicate should satisfied three conditions namely avoid the conflicts between search agents, movement towards the position of best search agent, and remains close to the best search agent. Whereas, the swarm behavior will update the positions of other search agents about the best optimal solution. The mathematical modeling of these behaviors is described in the preceding subsections.

#### 3.1.1. Avoiding the conflicts among search agents

To avoid the conflicts between search agents (i.e., other tunicates), vector $\vec{A}$ is employed for the calculation of new search agent position as shown in Fig. 2.

$$\vec{A} = \frac{\vec{G}}{\vec{M}} \tag{1}$$

$$\vec{G} = c_2 + c_3 - \vec{F} \tag{2}$$

$$\vec{F} = 2 \cdot c_1 \tag{3}$$

However, $\vec{G}$ is the gravity force and $\vec{F}$ shows the water flow advection in deep ocean. The variables $c_1, c_2$, and $c_3$ are random numbers lie in the range of $[0, 1]$. $\vec{M}$ represents the social forces between search agents. The vector $\vec{M}$ is calculated as follows:

$$\vec{M} = \left\lfloor P_{min} + c_1 \cdot P_{max} - P_{min} \right\rfloor \tag{4}$$

where $P_{min}$ and $P_{max}$ represent the initial and subordinate speeds to make social interaction. In this work, the values of $P_{min}$ and $P_{max}$ are considered as 1 and 4, respectively. Note that the detailed sensitivity analysis of these parameters is discussed in Section 5.5.

#### 3.1.2. Movement towards the direction of best neighbour

After avoiding the conflict between neighbors, the search agents are move towards the direction of best neighbour (see Fig. 3).

$$\vec{PD} = | \vec{FS} - r_{and} \cdot \vec{P_p}(x) | \tag{5}$$

where $\vec{PD}$ is the distance between the food source and search agent, i.e., tunicate, $x$ indicates the current iteration, $\vec{FS}$ is the position of food source, i.e., optimum. Vector $\vec{P_p}(x)$ indicates the position of tunicate and $r_{and}$ is a random number in range $[0, 1]$.

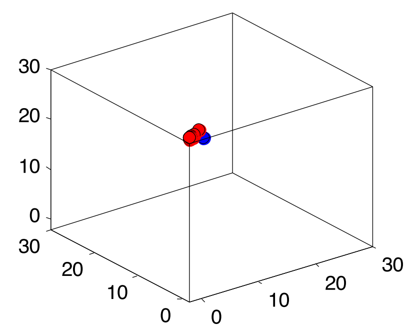


**Fig. 4.** Converge towards position of best search agent.

#### 3.1.3. Converge towards the best search agent

The search agent can maintain its position towards the best search agent (i.e., food source) which is shown in Fig. 4.

$$\vec{P_p}(x) = \begin{cases} \vec{FS} + \vec{A} \cdot \vec{PD}, & \text{if } r_{and} \geq 0.5 \\ \vec{FS} - \vec{A} \cdot \vec{PD}, & \text{if } r_{and} < 0.5 \end{cases} \tag{6}$$

where $\vec{P_p}(x')$ is the updated position of tunicate with respect to the position of food source $\vec{FS}$.

#### 3.1.4. Swarm behavior

In order to mathematically simulate the swarm behavior of tunicate, the first two optimal best solutions are saved and update the positions of other search agents according to the position of the best search agents. The following formula is proposed to define the swarm behavior of tunicate:

$$P_p(\vec{x} + 1) = \frac{\vec{P_p}(x) + P_p(\vec{x} + 1)}{2 + c_1} \tag{7}$$

Fig. 5 shows how search agents can updates their positions according to the position of $\vec{P}_p(x)$. The final position would be in a random place, within a cylindrical or cone-shaped, which is defined by the position of tunicate. The pseudo code of the proposed TSA algorithm is shown in Algorithm 1. There are some important points about the TSA algorithm which are described as:

- $\vec{A}$, $\vec{G}$, and $\vec{F}$ assist the solutions to behave randomly in a given search space and responsible to avoid the conflicts between different search agents.
- The possibility of better exploration and exploitation phases is done by the variations in vectors $\vec{A}$, $\vec{G}$, and $\vec{F}$.
- The jet propulsion and swarm behaviors of tunicate in a given search space defines the collective behavior of TSA algorithm (see Fig. 6).

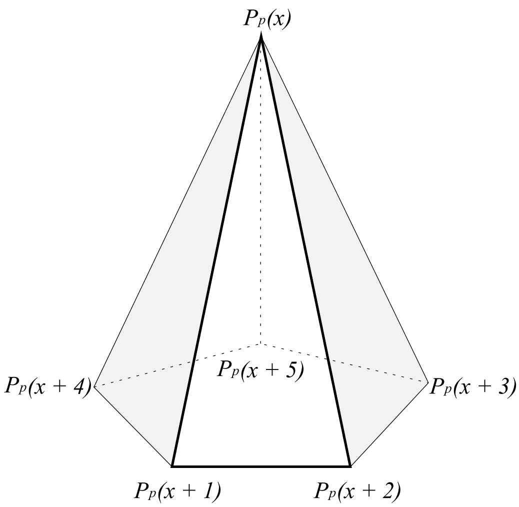


**Fig. 5.** 3D position vectors of tunicate.

### 3.2. Steps and flowchart of TSA

The steps and flowchart (see Fig. 7) of the proposed TSA are given below.

**Step 1:** Initialize the tunicate population $\vec{P}_p$.

**Step 2:** Choose the initial parameters and maximum number of iterations.

**Step 3:** Calculate the fitness value of each search agent.

**Step 4:** After computing the fitness value, the best search agent is explored in the given search space.

**Step 5:** Update the position of each search agent using Eq. (7).

**Step 6:** Adjust the updated search agent which goes beyond the boundary in a given search space.

**Step 7:** Compute the updated search agent fitness value. If there is a better solution than the previous optimal solution, then update $P_p$.

**Step 8:** If the stopping criterion is satisfied, then the algorithm stops. Otherwise, repeat the Steps 5–8.

**Step 9:** Return the best optimal solution which is obtained so far.

### 3.3. Computational complexity

In this subsection, the computational complexity of proposed TSA algorithm is discussed. Both the time and space complexities of the proposed algorithm are given below.

#### 3.3.1. Time complexity

1. The initialization of population process needs $\mathcal{O}(n \times d)$ time, where $n$ is the population size and $d$ defines the dimension of a given test problem.
2. The agent fitness needs $\mathcal{O}(Max_{iterations} \times n \times d)$ time, where $Max_{iterations}$ is the maximum number of iterations.
3. TSA requires $\mathcal{O}(N)$ time, where $N$ defines the jet propulsion and swarm behaviors of tunicate for better exploration and exploitation.

Hence, the total time complexity of TSA algorithm is $\mathcal{O}(Max_{iterations} \times n \times d \times N)$.

#### 3.3.2. Space complexity

The space complexity of TSA algorithm is $\mathcal{O}(n \times d)$, which is considered as the maximum amount of space during its initialization process.

## 4. Experimental results and discussions

This section describes the simulation and experimentation of TSA on seventy-four standard benchmark test functions. The detailed description of these benchmark test functions are discussed below. Further, the results are analyzed and compared with well-known metaheuristics.

### 4.1. Description of benchmark test functions

The seventy-four benchmark test functions are applied on the proposed algorithm to demonstrate its applicability and efficiency. These functions are divided into six main categories: Unimodal

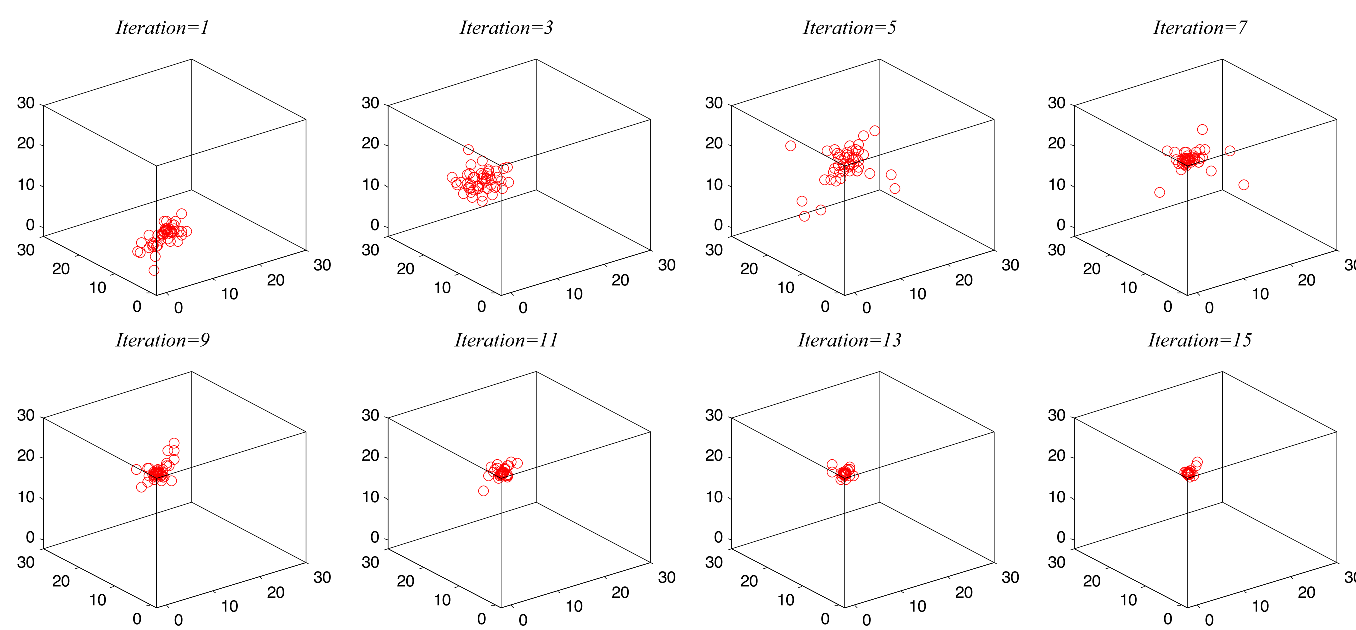


**Fig. 6.** Jet propulsion and swarm behaviors of tunicate in two-dimensional environment.

**Algorithm 1** Tunicate Swarm Algorithm

```
Input: Tunicate population P_p
Output: Optimal fitness value FS
procedure TSA
Initialize the parameters A, G, F, M, and Max_iterations
    Set P_min ← 1
    Set P_max ← 4
    Set Swarm ← 0
    while (x < Max_iterations) do
        for i ← 1 to 2 do      /* Looping for compute swarm behavior */
            FS ← ComputeFitness(P_p)      /* Calculate the fitness values of each search agent using ComputeFitness function*/
/* Jet propulsion behavior */
            c_1, c_2, c_3, r_and ← Rand()      /* Rand() is a function to generate the random number in range [0, 1] */
            M ← ⌊P_min + c_1 × P_max − P_min⌋
            F ← 2 × c_1
            G ← c_2 + c_3 − F
            A ← G/M
            PD ← ABS(FS − r_and × P_p(x))
/* Swarm behavior */
            if(r_and ≤ 0.5) then
                Swarm ← Swarm + FS + A × PD
            else
                Swarm ← Swarm + FS − A × PD
            end if
        end for
        P_p(x) ← Swarm/(2 + c_1)
        Swarm ← 0
        Update the parameters A, G, F, and M
        x ← x + 1
    end while
return FS
end procedure

procedure ComputeFitness(P_p)
    for i ← 1 to n do      /* Here, n represents the dimension of a given problem */
        FIT_p[i] ← FitnessFunction(P_p(i, :))      /* Calculate the fitness of each individual */
    end for
    FIT_pbest ← BEST(FIT_p[])      /* Calculate the best fitness value using BEST function */
return FIT_pbest
end procedure

procedure BEST(FIT_p)
    Best ← FIT_p[0]
    for i ← 1 to n do
        if(FIT_p[i] < Best) then
            Best ← FIT_p[i]
        end if
    end for
return Best      /* Return the best fitness value */
end procedure
```

(Digalakis and Margaritis, 2001), Multimodal (Yang, 2010), Fixed-dimension Multimodal (Digalakis and Margaritis, 2001; Yang, 2010), Composite (Liang et al., 2005), CEC-2015 (Chen et al., 2014), and CEC-2017 (Awad et al., 2016) test functions. The description of these test functions is given in Appendix.

### 4.2. Experimental setup

The proposed TSA is compared with well-known metaheuristic algorithms namely Spotted Hyena Optimizer (SHO) (Dhiman and Kumar, 2017), Grey Wolf Optimizer (GWO) (Mirjalili et al., 2014), Particle Swarm Optimization (PSO) (Kennedy and Eberhart, 1995), Multi-verse Optimizer (MVO) (Mirjalili et al., 2016), Sine Cosine Algorithm (SCA) (Mirjalili, 2016), Gravitational Search Algorithm (GSA) (Rashedi et al., 2009), Genetic Algorithm (GA) (Holland, 1992), Emperor Penguin Optimizer (EPO) (Dhiman and Kumar, 2018b), and jSO (Brest et al., 2017). Table 1 shows the parameter settings of all algorithms. The experimentation has been done on Matlab R2017b version using 64 bit Core i5 processor with 3.20 GHz and 16 GB main memory.

### 4.3. Performance comparison

The performance of proposed TSA algorithm is compared with state-of-the-art optimization algorithms on unimodal, multimodal, fixed-dimension multimodal, composite, CEC-2015, and CEC-2017 benchmark test functions. The average and standard deviation is considered

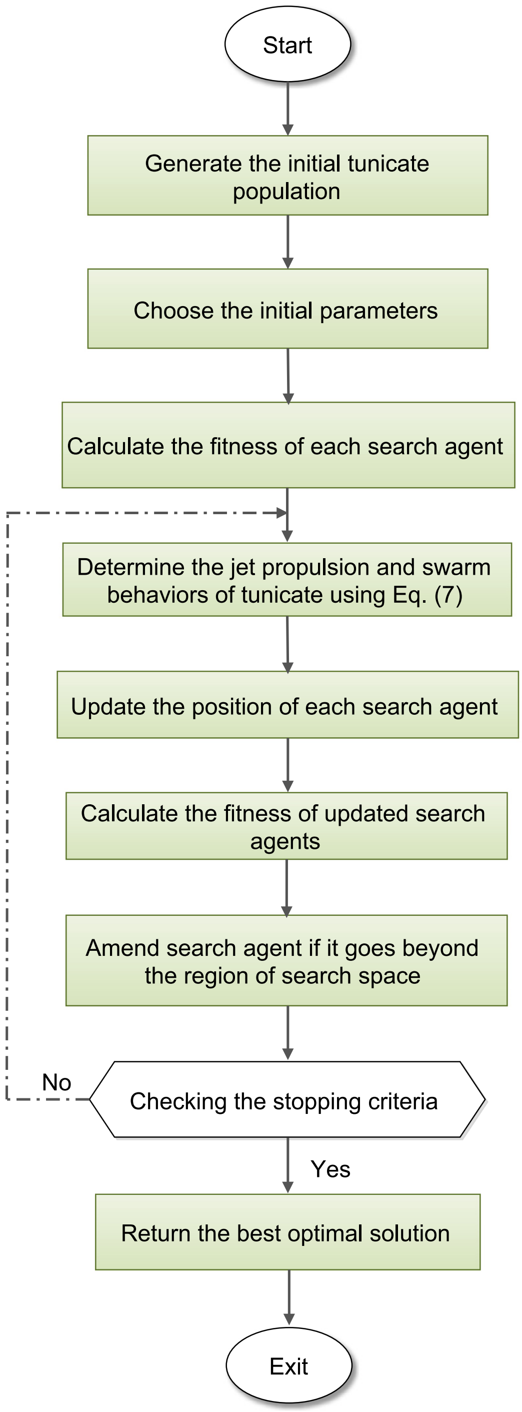


**Fig. 7.** Flowchart of the proposed TSA algorithm.

as the best optimal solution on benchmark functions. For benchmark test functions, the proposed algorithm simulates 30 independent runs in which each run employs 1000 number of iterations.

#### 4.3.1. *Evaluation of test functions* $F_1 - F_7$

Table 2 shows the mean and standard deviation of best obtained optimal solution on unimodal benchmark test functions. For $F_1$, $F_2$, and $F_3$ benchmark test functions, SHO is the best optimizer whereas TSA is the second best optimizer in terms of average and standard deviation. TSA obtains better competitor results on $F_4$, $F_5$, $F_6$, and $F_7$ benchmark test functions. It is seen from results that TSA is very effective and competitive as compared with other metaheuristic algorithms.

**Table 1**
Parameters settings.

| # | Algorithms | Parameters | Values |
|---|---|---|---|
| 1. | Tunicate Swarm Algorithm (TSA) | Search agents | 80 |
| | | Parameter $P_{min}$ | 1 |
| | | Parameter $P_{max}$ | 4 |
| | | Number of generations | 1000 |
| 2. | Spotted Hyena Optimizer (SHO) | Search agents | 80 |
| | | Control parameter ($\vec{h}$) | [5, 0] |
| | | $\vec{M}$ constant | [0.5, 1] |
| | | Number of generations | 1000 |
| 3. | Grey Wolf Optimizer (GWO) | Search agents | 80 |
| | | Control parameter ($\vec{a}$) | [2, 0] |
| | | Number of generations | 1000 |
| 4. | Particle Swarm Optimization (PSO) | Number of particles | 80 |
| | | Inertia coefficient | 0.75 |
| | | Cognitive and social coeff | 1.8, 2 |
| | | Number of generations | 1000 |
| 5. | Multi-Verse Optimizer (MVO) | Search agents | 80 |
| | | Wormhole existence Prob. | [0.2, 1] |
| | | Traveling distance rate | [0.6, 1] |
| | | Number of generations | 1000 |
| 6. | Sine Cosine Algorithm (SCA) | Search agents | 80 |
| | | Number of elites | 2 |
| | | Number of generations | 1000 |
| 7. | Gravitational Search Algorithm (GSA) | Search agents | 80 |
| | | Gravitational constant | 100 |
| | | Alpha coefficient | 20 |
| | | Number of generations | 1000 |
| 8. | Genetic Algorithm (GA) | Population size | 80 |
| | | Crossover | 0.9 |
| | | Mutation | 0.05 |
| | | Number of generations | 1000 |
| 9. | Emperor Penguin Optimizer (EPO) | Search agents | 80 |
| | | Temperature profile ($T'$) | [1, 1000] |
| | | $\vec{A}$ constant | [−1.5, 1.5] |
| | | Function $S()$ | [0, 1.5] |
| | | Parameter $M$ | 2 |
| | | Parameter $f$ | [2, 3] |
| | | Parameter $l$ | [1.5, 2] |
| | | Number of generations | 1000 |

#### 4.3.2. *Evaluation of test functions* $F_8 - F_{23}$

Tables 3 and 4 show the computational performance of above-mentioned algorithms on multimodal benchmark test functions ($F_8 - F_{13}$) and fixed-dimension multimodal benchmark test functions ($F_{14} - F_{23}$), respectively. These tables show that TSA is able to find near optimal solution on nine benchmark test problems (i.e., $F_8, F_{10}, F_{13}, F_{14}, F_{15}, F_{17}, F_{18}, F_{19}$, and $F_{22}$). For $F_9, F_{11}$, and $F_{16}$ benchmark test functions, SHO provides near optimal results than TSA algorithm. TSA is the second best optimizer on these benchmark test functions. PSO generates best optimal solution for $F_{12}$ and $F_{20}$ benchmark test functions. For $F_{21}$ benchmark test function, GWO and TSA are the first and second best metaheuristic optimization algorithms, respectively. The results show that TSA obtains very competitive results in majority of the benchmark test problems.

#### 4.3.3. *Evaluation of test functions* $F_{24} - F_{29}$

Table 5 shows the experimental results on composite benchmark test functions. The results show that over 3 out of 6 benchmark functions, TSA obtains better than the other approaches. GSA obtains best optimal solution for $F_{24}$ benchmark test function. For $F_{28}$ and $F_{29}$ benchmark test functions, SHO provides better optimal results than TSA algorithm. However, TSA is the third best optimization algorithm for $F_{24}$, $F_{28}$, and $F_{29}$ benchmark test functions.

**Table 2**
Mean and standard deviation of best optimal solution for 30 independent runs on unimodal benchmark test functions.

| *F* | TSA | | SHO | | GWO | | PSO | | MVO | | SCA | | GSA | | GA | | EPO | |
|---|---|---|---|---|---|---|---|---|---|---|---|---|---|---|---|---|---|---|
| | *Ave* | *Std* | *Ave* | *Std* | *Ave* | *Std* | *Ave* | *Std* | *Ave* | *Std* | *Ave* | *Std* | *Ave* | *Std* | *Ave* | *Std* | *Ave* | *Std* |
| $F_1$ | 7.71E−38 | 7.00E−21 | **0.00E+00** | **0.00E+00** | 4.61E−23 | 7.37E−23 | 4.98E−09 | 1.40E−08 | 2.81E−01 | 1.11E−01 | 3.55E−02 | 1.06E−01 | 1.16E−16 | 6.10E−17 | 1.95E−12 | 2.01E−11 | 5.71E−28 | 8.31E−29 |
| $F_2$ | 8.48E−39 | 5.92E−41 | **0.00E+00** | **0.00E+00** | 1.20E−34 | 1.30E−34 | 7.29E−04 | 1.84E−03 | 3.96E−01 | 1.41E−01 | 3.23E−05 | 8.57E−05 | 1.70E−01 | 9.29E−01 | 6.53E−18 | 5.10E−17 | 6.20E−40 | 3.32E−40 |
| $F_3$ | 1.15E−21 | 6.70E−21 | **0.00E+00** | **0.00E+00** | 1.00E−14 | 4.10E−14 | 1.40E+01 | 7.13E+00 | 4.31E+01 | 8.97E+00 | 4.91E+03 | 3.89E+03 | 4.16E+02 | 1.56E+02 | 7.70E−10 | 7.36E−09 | 2.05E−19 | 9.17E−20 |
| $F_4$ | **1.33E−23** | **1.15E−22** | 7.78E−12 | 8.96E−12 | 2.02E−14 | 2.43E−14 | 6.00E−01 | 1.72E−01 | 8.80E−01 | 2.50E−01 | 1.87E+01 | 8.21E+00 | 1.12E+00 | 9.89E−01 | 9.17E+01 | 5.67E+01 | 4.32E−18 | 3.98E−19 |
| $F_5$ | **5.13E+00** | **4.76E−03** | 8.59E+00 | 5.53E−01 | 2.79E+01 | 1.84E+00 | 4.93E+01 | 3.89E+01 | 1.18E+02 | 1.43E+02 | 7.37E+02 | 1.98E+03 | 3.85E+01 | 3.47E+01 | 5.57E+02 | 4.16E+01 | 5.07E+00 | 4.90E−01 |
| $F_6$ | **7.10E−21** | **1.12E−25** | 2.46E−01 | 1.78E−01 | 6.58E−01 | 3.38E−01 | 9.23E−09 | 1.78E−08 | 3.15E−01 | 9.98E−02 | 4.88E+00 | 9.75E−01 | 1.08E−16 | 4.00E−17 | 3.15E−01 | 9.98E−02 | 7.01E−19 | 4.39E−20 |
| $F_7$ | **3.72E−07** | **5.09E−07** | 3.29E−05 | 2.43E−05 | 7.80E−04 | 3.85E−04 | 6.92E−02 | 2.87E−02 | 2.02E−02 | 7.43E−03 | 3.88E−02 | 5.79E−02 | 7.68E−01 | 2.77E+00 | 6.79E−04 | 3.29E−03 | 2.71E−05 | 9.26E−06 |

**Table 3**
Mean and standard deviation of best optimal solution for 30 independent runs on multimodal benchmark test functions.

| *F* | TSA | | SHO | | GWO | | PSO | | MVO | | SCA | | GSA | | GA | | EPO | |
|---|---|---|---|---|---|---|---|---|---|---|---|---|---|---|---|---|---|---|
| | *Ave* | *Std* | *Ave* | *Std* | *Ave* | *Std* | *Ave* | *Std* | *Ave* | *Std* | *Ave* | *Std* | *Ave* | *Std* | *Ave* | *Std* | *Ave* | *Std* |
| $F_8$ | **−8.93E+02** | 4.15E+01 | −1.16E+02 | **2.72E+01** | −6.14E+02 | 9.32E+01 | −6.01E+02 | 1.30E+02 | −6.92E+02 | 9.19E+01 | −3.81E+02 | 2.83E+01 | −2.75E+02 | 5.72E+01 | −5.11E+02 | 4.37E+01 | −8.76E+02 | 5.92E+01 |
| $F_9$ | 5.70E−03 | 1.46E−03 | **0.00E+00** | **0.00E+00** | 4.34E−01 | 1.66E+00 | 4.72E+01 | 1.03E+01 | 1.01E+02 | 1.89E+01 | 2.23E+01 | 3.25E+01 | 3.35E+01 | 1.19E+01 | 1.23E−01 | 4.11E+01 | 6.90E−01 | 4.81E−01 |
| $F_{10}$ | **9.80E−19** | 4.51E−12 | 2.48E+00 | 1.41E+00 | 1.63E−14 | **3.14E−15** | 3.86E−02 | 2.11E−01 | 1.15E+00 | 7.87E−01 | 1.55E+01 | 8.11E+00 | 8.25E−09 | 1.90E−09 | 5.31E−11 | 1.11E−10 | 8.03E−16 | 2.74E−14 |
| $F_{11}$ | 1.00E−07 | 7.46E−07 | **0.00E+00** | **0.00E+00** | 2.29E−03 | 5.24E−03 | 5.50E−03 | 7.39E−03 | 5.74E−01 | 1.12E−01 | 3.01E−01 | 2.89E−01 | 8.19E+00 | 3.70E+00 | 3.31E−06 | 4.23E−05 | 4.20E−05 | 4.73E−04 |
| $F_{12}$ | 6.07E−06 | 2.72E−05 | 3.68E−02 | 1.15E−02 | 3.93E−02 | 2.42E−02 | **1.05E−10** | **2.06E−10** | 1.27E+00 | 1.02E+00 | 5.21E+01 | 2.47E+02 | 2.65E−01 | 3.14E−01 | 9.16E−08 | 4.88E−07 | 5.09E−03 | 3.75E−03 |
| $F_{13}$ | **0.00E+00** | **0.00E+00** | 9.29E−01 | 9.52E−02 | 4.75E−01 | 2.38E−01 | 4.03E−03 | 5.39E−03 | 6.60E−02 | 4.33E−02 | 2.81E+02 | 8.63E+02 | 5.73E−32 | 8.95E−32 | 6.39E−02 | 4.49E−02 | 0.00E+00 | 0.00E+00 |

**Table 4**
Mean and standard deviation of best optimal solution for 30 independent runs on fixed-dimension multimodal benchmark test functions.

| $F$ | TSA | | SHO | | GWO | | PSO | | MVO | | SCA | | GSA | | GA | | EPO | |
|---|---|---|---|---|---|---|---|---|---|---|---|---|---|---|---|---|---|---|
| | *Ave* | *Std* | *Ave* | *Std* | *Ave* | *Std* | *Ave* | *Std* | *Ave* | *Std* | *Ave* | *Std* | *Ave* | *Std* | *Ave* | *Std* | *Ave* | *Std* |
| $F_{14}$ | **1.03E+00** | 2.11E−04 | 9.68E+00 | 3.29E+00 | 3.71E+00 | 3.86E+00 | 2.77E+00 | 2.32E+00 | 9.98E+01 | **9.14E−12** | 1.26E+00 | 6.86E−01 | 3.61E+00 | 2.96E+00 | 4.39E+00 | 4.41E−02 | 1.08E+00 | 4.11E−02 |
| $F_{15}$ | **8.10E−05** | **4.06E−05** | 9.01E−03 | 1.06E−03 | 3.66E−02 | 7.60E−02 | 9.09E−03 | 2.38E−03 | 7.15E−02 | 1.26E−01 | 1.01E−02 | 3.75E−03 | 6.84E−02 | 7.37E−02 | 7.36E−02 | 2.39E−03 | 8.21E−03 | 4.09E−03 |
| $F_{16}$ | −1.02E+00 | 1.99E−09 | **−1.03E+00** | **2.86E−11** | −1.02E+00 | 7.02E−09 | −1.02E+00 | 0.00E+00 | −1.02E+00 | 4.74E−08 | −1.02E+00 | 3.23E−05 | −1.02E+00 | 0.00E+00 | −1.02E+00 | 4.19E−07 | −1.02E+00 | 9.80E−07 |
| $F_{17}$ | **3.96E−01** | 3.71E−09 | 3.97E−01 | 2.46E−01 | 3.98E−01 | 7.00E−07 | 3.97E−01 | 9.03E−16 | 3.98E−01 | 1.15E−07 | 3.98E−01 | 7.61E−04 | 3.98E−01 | 1.13E−16 | 3.98E−01 | **3.71E−17** | 3.98E−01 | 5.39E−05 |
| $F_{18}$ | **3.00E+00** | **3.56E−09** | 3.00E+00 | 9.05E+00 | 3.00E+00 | 7.16E−06 | 3.00E+00 | 6.59E−05 | 3.00E+00 | 1.48E+01 | 3.00E+00 | 2.25E−05 | 3.00E+00 | 3.24E−02 | 3.00E+00 | 6.33E−07 | 3.00E+00 | 1.15E−08 |
| $F_{19}$ | **−3.89E+00** | 3.01E−09 | −3.71E+00 | 4.39E−01 | −3.84E+00 | 1.57E−03 | −3.80E+00 | **3.37E−15** | −3.77E+00 | 3.53E−07 | −3.75E+00 | 2.55E−03 | −3.86E+00 | 4.15E−01 | −3.81E+00 | 4.37E−10 | −3.86E+00 | 6.50E−07 |
| $F_{20}$ | −2.97E+00 | 2.10E−01 | −1.44E+00 | 5.47E−01 | −3.27E+00 | 7.27E−02 | **−3.32E+00** | 2.66E−01 | −3.23E+00 | **5.37E−02** | −2.84E+00 | 3.71E−01 | −1.47E+00 | 5.32E−01 | −2.39E+00 | 4.37E−01 | −2.81E+00 | 7.11E−01 |
| $F_{21}$ | −7.01E+00 | 1.23E+00 | −2.08E+00 | **3.80E−01** | **−9.65E+00** | 1.54E+00 | −7.54E+00 | 2.77E+00 | −7.38E+00 | 2.91E+00 | −2.28E+00 | 1.80E+00 | −4.57E+00 | 1.30E+00 | −5.19E+00 | 2.34E+00 | −8.07E+00 | 2.29E+00 |
| $F_{22}$ | **−13.07E+00** | 3.15E−03 | −1.61E+00 | **2.04E−04** | −1.04E+00 | 2.73E−04 | −8.55E+00 | 3.08E+00 | −8.50E+00 | 3.02E+00 | −3.99E+00 | 1.99E+00 | −6.58E+00 | 2.64E+00 | −2.97E+00 | 1.37E−02 | −10.01E+00 | 3.97E−02 |
| $F_{23}$ | −3.51E+00 | 3.10E−03 | −1.68E+00 | 2.64E−01 | **−1.05E+01** | **1.81E−04** | −9.19E+00 | 2.52E+00 | −8.41E+00 | 3.13E+00 | −4.49E+00 | 1.96E+00 | −9.37E+00 | 2.75E+00 | −3.10E+00 | 2.37E+00 | −3.41E+00 | 1.11E−02 |

**Table 5**
Mean and standard deviation of best optimal solution for 30 independent runs on composite benchmark test functions.

| *F* | TSA | | SHO | | GWO | | PSO | | MVO | | SCA | | GSA | | GA | | EPO | |
|---|---|---|---|---|---|---|---|---|---|---|---|---|---|---|---|---|---|---|
| | *Ave* | *Std* | *Ave* | *Std* | *Ave* | *Std* | *Ave* | *Std* | *Ave* | *Std* | *Ave* | *Std* | *Ave* | *Std* | *Ave* | *Std* | *Ave* | *Std* |
| $F_{24}$ | 1.33E+02 | 4.10E+01 | 2.30E+02 | 1.37E+02 | 8.39E+01 | 8.42E+01 | 6.00E+01 | 8.94E+01 | 1.40E+02 | 1.52E+02 | 1.20E+02 | 3.11E+01 | **4.49E−17** | **2.56E−17** | 5.97E+02 | 1.34E+02 | 2.33E+02 | 9.22E+01 |
| $F_{25}$ | **3.00E+01** | 2.02E+01 | 4.08E+02 | 9.36E+01 | 1.48E+02 | 3.78E+01 | 2.44E+02 | 1.73E+02 | 2.50E+02 | 1.44E+02 | 1.14E+02 | **1.84E+00** | 2.03E+02 | 4.47E+02 | 4.09E+02 | 2.10E+01 | 4.10E+01 | 3.09E+01 |
| $F_{26}$ | **3.34E+02** | 4.36E+01 | 3.39E+02 | **3.14E+01** | 3.53E+02 | 5.88E+01 | 3.39E+02 | 8.36E+01 | 4.05E+02 | 1.67E+02 | 3.89E+02 | 5.41E+01 | 3.67E+02 | 8.38E+01 | 9.30E+02 | 8.31E+01 | 3.39E+02 | 5.03E+01 |
| $F_{27}$ | **2.40E+02** | **1.13E+01** | 7.26E+02 | 1.21E+02 | 4.23E+02 | 1.14E+02 | 4.49E+02 | 1.42E+02 | 3.77E+02 | 1.28E+02 | 4.31E+02 | 2.94E+01 | 5.32E+02 | 1.01E+02 | 4.97E+02 | 3.24E+01 | 3.44E+02 | 2.17E+01 |
| $F_{28}$ | 1.20E+02 | 4.00E+01 | **1.06E+02** | **1.38E+01** | 1.36E+02 | 2.13E+02 | 2.40E+02 | 4.25E+02 | 2.45E+02 | 9.96E+01 | 1.56E+02 | 8.30E+01 | 1.44E+02 | 1.31E+02 | 1.90E+02 | 5.03E+01 | 1.46E+02 | 7.06E+01 |
| $F_{29}$ | 6.41E+02 | 6.00E+02 | **5.97E+02** | **4.98E+00** | 8.26E+02 | 1.74E+02 | 8.22E+02 | 1.80E+02 | 8.33E+02 | 1.68E+02 | 6.06E+02 | 1.66E+02 | 8.13E+02 | 1.13E+02 | 6.65E+02 | 3.37E+02 | 7.43E+02 | 9.09E+02 |

**Table 6**
Mean and standard deviation of best optimal solution for 30 independent runs on CEC-2015 benchmark test functions.

| *F* | TSA | | SHO | | GWO | | PSO | | MVO | | SCA | | GSA | | GA | | EPO | |
|---|---|---|---|---|---|---|---|---|---|---|---|---|---|---|---|---|---|---|
| | *Ave* | *Std* | *Ave* | *Std* | *Ave* | *Std* | *Ave* | *Std* | *Ave* | *Std* | *Ave* | *Std* | *Ave* | *Std* | *Ave* | *Std* | *Ave* | *Std* |
| $CEC-1$ | **1.24E+05** | 1.13E+06 | 2.28E+06 | 2.18E+06 | 2.02E+06 | 2.08E+06 | 4.37E+05 | **4.73E+05** | 1.47E+06 | 2.63E+06 | 6.06E+05 | 5.02E+05 | 7.65E+06 | 3.07E+06 | 3.20E+07 | 8.37E+06 | 1.50E+05 | 1.21E+06 |
| $CEC-2$ | 5.55E+05 | 1.00E+06 | 3.13E+05 | 4.19E+05 | 5.65E+06 | 6.03E+06 | 9.41E+03 | 1.08E+04 | 1.97E+04 | 1.46E+04 | 1.43E+04 | 1.03E+04 | 7.33E+08 | 2.33E+08 | **4.58E+03** | **1.09E+03** | 6.70E+06 | 1.34E+08 |
| $CEC-3$ | **3.20E+02** | 2.36E−03 | 3.20E+02 | 3.76E−02 | 3.20E+02 | 7.08E−02 | 3.20E+02 | 8.61E−02 | 3.20E+02 | 9.14E−02 | 3.20E+02 | 3.19E−02 | 3.20E+02 | 7.53E−02 | 3.20E+02 | **1.11E−05** | 3.20E+02 | 1.16E−03 |
| $CEC-4$ | 5.70E+02 | 3.30E+01 | 4.11E+02 | 1.71E+01 | 4.16E+02 | 1.03E+01 | **4.09E+02** | **3.96E+00** | 4.26E+02 | 1.17E+01 | 4.18E+02 | 1.03E+01 | 4.42E+02 | 7.72E+00 | 4.39E+02 | 7.25E+00 | 4.10E+02 | 5.61E+01 |
| $CEC-5$ | 8.75E+02 | 3.18E+02 | 9.13E+02 | 1.85E+02 | 9.20E+02 | **1.78E+02** | **8.65E+02** | 2.16E+02 | 1.33E+03 | 3.45E+02 | 1.09E+03 | 2.81E+02 | 1.76E+03 | 2.30E+02 | 1.75E+03 | 2.79E+02 | 9.81E+02 | 2.06E+02 |
| $CEC-6$ | 2.10E+03 | 1.28E+04 | 1.29E+04 | 1.15E+04 | 2.26E+04 | 2.45E+04 | **1.86E+03** | **1.93E+03** | 7.35E+03 | 3.82E+03 | 3.82E+03 | 2.44E+03 | 2.30E+04 | 2.41E+04 | 3.91E+06 | 2.70E+06 | 2.05E+03 | 1.05E+04 |
| $CEC-7$ | **7.02E+02** | **3.17E−02** | 7.02E+02 | 6.76E−01 | 7.02E+02 | 7.07E−01 | 7.02E+02 | 7.75E−01 | 7.02E+02 | 1.10E+00 | 7.02E+02 | 9.40E−01 | 7.06E+02 | 9.07E−01 | 7.08E+02 | 1.32E+00 | 7.02E+02 | 5.50E−01 |
| $CEC-8$ | **1.41E+03** | 1.01E+03 | 1.86E+03 | 1.98E+03 | 3.49E+03 | 2.04E+03 | 3.43E+03 | 2.77E+03 | 9.93E+03 | 8.74E+03 | 2.58E+03 | **1.61E+03** | 6.73E+03 | 3.36E+03 | 6.07E+05 | 4.81E+05 | 1.47E+03 | 2.34E+03 |
| $CEC-9$ | **1.00E+03** | 1.65E+01 | 1.00E+03 | 1.43E−01 | 1.00E+03 | 1.28E−01 | 1.00E+03 | 7.23E−02 | 1.00E+03 | 2.20E−01 | 1.00E+03 | **5.29E−02** | 1.00E+03 | 9.79E−01 | 1.00E+03 | 5.33E+00 | 1.00E+03 | 1.51E+01 |
| $CEC-10$ | **1.19E+03** | 4.42E+04 | 2.00E+03 | 2.73E+03 | 4.00E+03 | 2.82E+03 | 3.27E+03 | 1.84E+03 | 8.39E+03 | 1.12E+04 | 2.62E+03 | **1.78E+03** | 9.91E+03 | 8.83E+03 | 3.42E+05 | 1.74E+05 | 1.23E+03 | 2.51E+04 |
| $CEC-11$ | **1.34E+03** | **1.21E+01** | 1.38E+03 | 2.42E+01 | 1.40E+03 | 5.81E+01 | 1.35E+03 | 1.12E+02 | 1.37E+03 | 8.97E+01 | 1.39E+03 | 5.42E+01 | 1.35E+03 | 1.11E+02 | 1.41E+03 | 7.73E+01 | 1.35E+03 | 1.41E+01 |
| $CEC-12$ | **1.30E+03** | 5.35E+00 | 1.30E+03 | 7.89E−01 | 1.30E+03 | **6.69E−01** | 1.30E+03 | 6.94E−01 | 1.30E+03 | 9.14E−01 | 1.30E+03 | 8.07E−01 | 1.31E+03 | 1.54E+00 | 1.31E+03 | 2.05E+00 | 1.30E+03 | 7.50E+00 |
| $CEC-13$ | **1.30E+03** | **4.40E−07** | 1.30E+03 | 2.76E−04 | 1.30E+03 | 1.92E−04 | 1.30E+03 | 5.44E−03 | 1.30E+03 | 1.04E−03 | 1.30E+03 | 2.43E−04 | 1.30E+03 | 3.78E−03 | 1.35E+03 | 4.70E+01 | 1.30E+03 | 6.43E−05 |
| $CEC-14$ | **3.16E+03** | 1.76E+03 | 4.25E+03 | 1.73E+03 | 7.29E+03 | 2.45E+03 | 7.10E+03 | 3.12E+03 | 7.60E+03 | 1.29E+03 | 7.34E+03 | 2.47E+03 | 7.51E+03 | 1.52E+03 | 9.30E+03 | **4.04E+02** | 3.22E+03 | 2.12E+03 |
| $CEC-15$ | **1.60E+03** | 3.45E+01 | 1.60E+03 | 3.76E+00 | 1.61E+03 | 4.94E+00 | 1.60E+03 | **2.66E−07** | 1.61E+03 | 1.13E+01 | 1.60E+03 | 1.80E−02 | 1.62E+03 | 3.64E+00 | 1.64E+03 | 1.12E+01 | 1.60E+03 | 5.69E+01 |

**Table 7**
Mean and standard deviation of best optimal solution for 30 independent runs on CEC-2017 benchmark test functions.

| *F* | TSA | | SHO | | GWO | | PSO | | MVO | | SCA | | GSA | | GA | | jSO | |
|---|---|---|---|---|---|---|---|---|---|---|---|---|---|---|---|---|---|---|
| | *Ave* | *Std* | *Ave* | *Std* | *Ave* | *Std* | *Ave* | *Std* | *Ave* | *Std* | *Ave* | *Std* | *Ave* | *Std* | *Ave* | *Std* | *Ave* | *Std* |
| $C-1$ | 2.70E+04 | 1.21E+07 | 2.38E+05 | 2.28E+07 | 2.12E+05 | 2.18E+07 | 4.47E+04 | 4.83E+06 | 1.57E+05 | 2.73E+07 | 6.16E+04 | 5.12E+06 | 7.75E+05 | 3.17E+07 | 3.30E+06 | 8.47E+07 | **0.00E+00** | **0.00E+00** |
| $C-2$ | 5.82E+05 | 3.41E+09 | 3.23E+04 | 4.29E+06 | 5.75E+05 | 6.13E+07 | 9.51E+03 | 1.18E+05 | 1.07E+03 | 1.56E+05 | 1.53E+04 | 1.13E+05 | 7.43E+07 | 2.43E+09 | 4.68E+03 | 1.19E+04 | **0.00E+00** | **0.00E+00** |
| $C-3$ | 3.30E+02 | 2.38E−05 | 3.30E+02 | 3.86E−03 | 3.30E+02 | 7.18E−03 | 3.30E+02 | 8.71E−03 | 3.30E+02 | 9.24E−03 | 3.30E+02 | 3.29E−03 | 3.30E+02 | 7.63E−03 | 3.30E+02 | 1.21E−06 | **0.00E+00** | **0.00E+00** |
| $C-4$ | **3.40E+01** | 4.62E+02 | 4.21E+02 | 1.81E+02 | 4.26E+02 | 1.13E+02 | 4.19E+02 | 3.06E+01 | 4.36E+02 | 1.27E+02 | 4.28E+02 | 1.13E+02 | 4.52E+02 | 7.82E+02 | 4.49E+02 | 7.35E+02 | 5.62E+01 | **4.88E+01** |
| $C-5$ | **1.40E+01** | 2.19E+03 | 9.23E+02 | 1.95E+03 | 9.30E+02 | 1.88E+03 | 8.75E+02 | 2.26E+03 | 1.43E+04 | 3.55E+04 | 1.19E+04 | 2.91E+03 | 1.86E+03 | 2.40E+03 | 1.85E+03 | 2.89E+03 | 1.64E+01 | **3.46E+00** |
| $C-6$ | 2.17E+04 | 2.13E+05 | 1.39E+04 | 1.25E+05 | 2.36E+03 | 2.55E+05 | 1.96E+03 | 1.03E+04 | 7.45E+03 | 3.92E+04 | 3.92E+04 | 2.54E+04 | 2.40E+04 | 2.51E+05 | 3.01E+05 | 2.80E+07 | **1.09E−06** | **2.62E−06** |
| $C-7$ | 7.12E+02 | **4.49E−02** | 7.12E+02 | 6.86E−02 | 7.12E+02 | 7.17E−02 | 7.12E+03 | 7.85E−02 | 7.12E+02 | 1.20E+01 | 7.12E+03 | 9.50E−02 | 7.16E+02 | 9.17E−02 | 7.18E+02 | 1.42E+01 | **6.65E+01** | 3.47E+00 |
| $C-8$ | **1.56E+01** | 3.00E+04 | 1.96E+03 | 1.08E+04 | 3.59E+04 | 2.14E+04 | 3.53E+03 | 2.87E+04 | 9.03E+03 | 8.84E+05 | 2.68E+04 | 1.71E+04 | 6.83E+03 | 3.46E+04 | 6.17E+04 | 4.91E+08 | 1.70E+01 | **3.14E+00** |
| $C-9$ | 1.10E+03 | 1.50E+02 | 1.10E+04 | 1.53E−02 | 1.10E+04 | 1.38E−02 | 1.10E+03 | 7.33E−02 | 1.10E+04 | 2.30E−01 | 1.10E+03 | 5.39E−03 | 1.10E+03 | 9.89E−02 | 1.10E+04 | 5.43E+01 | **0.00E+00** | **0.00E+00** |
| $C-10$ | **1.32E+03** | 1.50E+04 | 2.10E+03 | 2.83E+04 | 4.10E+04 | 2.92E+04 | 3.37E+03 | 1.94E+04 | 8.49E+04 | 1.22E+05 | 2.72E+03 | 1.88E+04 | 9.01E+04 | 8.93E+04 | 3.52E+04 | 1.84E+06 | 3.14E+03 | **3.67E+02** |
| $C-11$ | **1.45E+01** | 2.76E+01 | 1.48E+03 | 2.52E+02 | 1.50E+04 | 5.91E+02 | 1.45E+03 | 1.22E+03 | 1.47E+04 | 8.07E+02 | 1.49E+04 | 5.52E+02 | 1.45E+04 | 1.21E+03 | 1.51E+03 | 7.83E+02 | 2.79E+01 | **3.33E+00** |
| $C-12$ | **1.40E+03** | 6.79E+00 | 1.40E+04 | 7.99E−02 | 1.40E+03 | **6.79E−02** | 1.40E+04 | 6.04E−02 | 1.40E+03 | 9.24E−02 | 1.40E+05 | 8.17E−02 | 1.41E+03 | 1.64E+01 | 1.41E+06 | 2.15E+01 | 1.68E+03 | 5.23E+02 |
| $C-13$ | **1.40E+01** | **5.49E−06** | 1.40E+02 | 2.86E−05 | 1.40E+06 | 1.02E−05 | 1.40E+03 | 5.54E−04 | 1.40E+04 | 1.14E−04 | 1.40E+03 | 2.53E−05 | 1.40E+04 | 3.88E−04 | 1.45E+02 | 4.80E+02 | 3.06E+01 | 2.12E+01 |
| $C-14$ | 3.33E+03 | 2.00E+03 | 4.35E+04 | 1.83E+04 | 7.39E+03 | 2.55E+04 | 7.20E+03 | 3.22E+04 | 7.70E+04 | 1.39E+04 | 7.44E+04 | 2.57E+04 | 7.61E+03 | 1.62E+04 | 9.40E+03 | 4.14E+03 | **2.50E+01** | **1.87E+00** |
| $C-15$ | 1.70E+03 | 9.86E+01 | 1.70E+03 | 3.86E+01 | 1.71E+04 | 4.04E+01 | 1.70E+03 | **2.76E−05** | 1.71E+06 | 1.23E+02 | 1.70E+03 | 1.90E−03 | 1.72E+06 | 3.74E+01 | 1.74E+06 | 1.22E+01 | **2.39E+01** | 2.49E+00 |
| $C-16$ | 2.46E+04 | 3.20E+08 | 3.28E+05 | 3.18E+09 | 3.02E+06 | 3.08E+09 | 5.37E+05 | 5.73E+08 | 2.47E+05 | 3.63E+09 | 7.06E+05 | 6.02E+09 | 8.65E+05 | 4.07E+09 | 4.20E+06 | 9.37E+09 | **4.51E+02** | **1.38E+02** |
| $C-17$ | 8.48E+05 | 7.03E+06 | 4.13E+04 | 5.19E+04 | 6.65E+06 | 7.03E+05 | 8.41E+04 | 2.08E+04 | 2.97E+04 | 2.46E+04 | 2.43E+05 | 2.03E+03 | 8.33E+06 | 3.33E+07 | 5.58E+03 | 2.09E+03 | **2.83E+02** | **8.61E+01** |
| $C-18$ | 4.20E+02 | 7.47E−05 | 4.20E+02 | 4.76E−04 | 4.20E+02 | 8.08E−04 | 4.20E+02 | 9.61E−04 | 4.20E+02 | 8.14E−04 | 4.20E+03 | 4.19E−04 | 4.20E+02 | 8.53E−04 | 4.20E+03 | **2.11E−07** | **2.43E+01** | 2.02E+00 |
| $C-19$ | 4.05E+02 | 5.60E+02 | 5.11E+03 | 2.71E+02 | 5.16E+02 | 2.03E+02 | **1.09E+01** | **4.90E−01** | 5.26E+02 | 2.17E+02 | 5.18E+03 | 2.03E+02 | 5.42E+02 | 8.72E+02 | 5.39E+03 | 8.25E+02 | 1.41E+01 | 2.26E+00 |
| $C-20$ | **1.11E+02** | 4.07E+01 | 8.13E+03 | 2.85E+01 | 8.20E+02 | **2.78E+00** | 7.65E+02 | 3.16E+01 | 2.33E+03 | 4.45E+02 | 2.09E+03 | 3.81E+01 | 2.76E+04 | 3.30E+02 | 2.75E+03 | 3.79E+01 | 1.40E+02 | 7.74E+01 |
| $C-21$ | 3.02E+03 | 2.16E+04 | 2.29E+03 | 2.15E+04 | 3.26E+04 | 3.45E+05 | 2.86E+03 | 2.93E+03 | 8.35E+04 | 4.82E+03 | 4.82E+04 | 3.44E+04 | 3.30E+04 | 3.41E+04 | 4.91E+06 | 3.70E+07 | **2.19E+02** | **3.77E+00** |
| $C-22$ | **8.02E+02** | **5.47E−02** | 8.02E+02 | 7.76E−01 | 8.02E+03 | 8.07E−01 | 8.02E+02 | 8.75E−01 | 8.02E+02 | 2.10E+01 | 8.02E+03 | 8.40E−01 | 8.06E+03 | 8.07E−02 | 8.08E+02 | 2.32E+00 | 1.49E+03 | 1.75E+03 |
| $C-23$ | 3.35E+03 | 1.31E+03 | 2.86E+03 | 2.98E+04 | 4.49E+04 | 3.04E+04 | 4.43E+04 | 3.77E+04 | 8.93E+04 | 9.74E+04 | 3.58E+03 | 2.61E+04 | 7.73E+03 | 4.36E+04 | 7.07E+04 | 5.81E+06 | **4.30E+02** | **6.24E+00** |
| $C-24$ | 2.00E+04 | 6.76E+01 | 2.00E+04 | 2.43E−02 | 2.00E+04 | 2.28E−02 | 2.00E+04 | 7.23E−03 | 2.00E+04 | 3.20E−02 | 2.00E+04 | **6.29E−03** | 2.00E+04 | 8.79E−02 | 2.00E+04 | 6.33E+01 | **5.07E+02** | 4.13E+00 |
| $C-25$ | **2.22E+02** | 6.46E+05 | 3.00E+04 | 3.73E+04 | 5.00E+04 | 3.82E+04 | 4.27E+04 | 2.84E+04 | 9.39E+04 | 2.12E+05 | 3.62E+04 | 2.78E+04 | 8.91E+04 | 6.83E+04 | 4.42E+06 | 2.74E+06 | 4.81E+02 | **2.80E+00** |
| $C-26$ | **1.00E+03** | **2.26E+01** | 2.38E+04 | 3.42E+02 | 2.40E+04 | 6.81E+02 | 2.35E+05 | 2.12E+03 | 2.37E+04 | 9.97E+02 | 2.39E+04 | 6.42E+02 | 2.35E+04 | 2.11E+03 | 2.41E+04 | 8.73E+02 | 1.13E+03 | 5.62E+01 |
| $C-27$ | 2.30E+04 | 1.40E+00 | 2.30E+04 | 8.89E−02 | 2.30E+04 | **7.69E−02** | 2.30E+04 | 7.94E−02 | 2.30E+04 | 8.14E−02 | 2.30E+04 | 9.07E−02 | 2.31E+04 | 3.54E+01 | 2.31E+04 | 3.05E+00 | **5.11E+02** | 1.11E+01 |
| $C-28$ | 5.30E+04 | **6.11E−06** | 5.30E+04 | 3.76E−05 | 5.30E+04 | 3.92E−05 | 5.30E+04 | 6.44E−04 | 5.30E+04 | 2.04E−04 | 5.30E+04 | 3.43E−05 | 5.30E+04 | 4.78E−04 | 5.35E+04 | 4.70E+02 | **4.60E+02** | 6.84E+00 |
| $C-29$ | **3.20E+02** | 4.66E+03 | 5.25E+04 | 2.73E+04 | 8.29E+03 | 3.45E+04 | 8.10E+04 | 4.12E+04 | 8.60E+03 | 2.29E+05 | 8.34E+04 | 3.47E+05 | 8.51E+03 | 2.52E+04 | 8.30E+04 | 5.04E+03 | 3.63E+02 | **1.32E+01** |
| $C-30$ | **2.60E+04** | 5.55E+01 | 2.60E+04 | 4.76E+01 | 2.61E+04 | 5.94E+01 | 2.60E+04 | **3.66E−04** | 2.61E+04 | 2.13E+02 | 2.60E+04 | 2.80E−03 | 2.62E+04 | 4.64E+01 | 2.64E+04 | 2.12E+02 | 6.01E+05 | 2.99E+04 |

#### 4.3.4. Evaluation of IEEE CEC-2015 test functions (CEC1 – CEC15)

Table 6 reveals the performance of TSA and other optimization algorithms on IEEE CEC-2015 benchmark test functions. It is seen from Table 6 that TSA generates better results for $CEC-1, CEC-3, CEC-7, CEC-8, CEC-9, CEC-10, CEC-11, CEC-12, CEC-13, CEC-14$, and $CEC-15$ benchmark test functions. For $CEC-4, CEC-5$, and $CEC-6$ benchmark test functions, PSO performance is better than other algorithms in terms of fitness value. TSA is the second best optimizer on these test functions.

#### 4.3.5. Evaluation of IEEE CEC-2017 test functions (C1–C30)

Table 7 reveals the performance of proposed TSA algorithm and other competitive algorithms on IEEE CEC-2017 benchmark test functions. The results show that TSA generates best optimal solution for $C-4, C-5, C-8, C-10, C-11, C-12, C-13, C-20, C-22, C-25, C-26, C-29, C-30$ benchmark test functions.

### 4.4. Convergence analysis

The convergence curves of proposed TSA algorithm is shown in Fig. 8. It is analyzed that TSA is very competitive over benchmark functions. TSA algorithm has three different behaviors of convergence. In the starting stage of iteration process, the convergence efficiency of TSA algorithm is more quickly in a given search space. In second stage of iteration, TSA converges with the direction of optimum when final iteration reaches. The last iteration process shows the express convergence behavior from the initial stage of iterations. The results show that TSA algorithm maintains a balance between exploration and exploitation. The search history is another metric to determine how TSA explores and exploits in a given search space. The search history of TSA is depicted in Fig. 8. It is observed from Fig. 8 that TSA explore most promising area in the given search space for benchmark test functions. For unimodal test functions, the sample points are sparsely distributed in the non-promising area. Whereas, the most of sample points are distributed around the promising area for multimodal and fixed-dimension multimodal test functions. This is due to the difficulty level of these test functions. TSA does not stuck in local optima and explores the entire search space. The distribution of sample points is around the true optimal solution, which ensures its exploitation capability. Therefore, TSA has both exploration and exploitation capability.

### 4.5. Sensitivity analysis

The proposed TSA algorithm employs four parameters, i.e., maximum number of iterations, number of search agents, parameter $P_{min}$, and parameter $P_{max}$.

1. Maximum number of iterations: TSA algorithm was simulate for different number of iteration processes. The values of $Max_{iteration}$ used in this work are 100, 500, 800, and 1000. Table 8 and Fig. 9(a) show the variations of iterations on various benchmark test functions. The results show that TSA converges towards the optimal solution when the number of iterations is increased.
2. Number of search agents: TSA algorithm was simulate for different values of search agent (i.e., 30, 50, 80, 100). Table 9 and Fig. 9(b) show the variations of different number of search agents on benchmark test functions. It is analyzed from Fig. 9(b) that the value of fitness function decreases when number of search agents increases.
3. Variation in parameter $P_{min}$: To investigate the effect of parameter $P_{min}$, TSA algorithm was run for different values of $P_{min}$ keeping other parameters fixed. The values of $P_{min}$ used in experimentation are 1, 2, 3, and 4. Table 10 and Fig. 9(c) show the variation of $P_{min}$ on different benchmark test functions. The results show that TSA generates better optimal results when the value of $P_{min}$ is set to 1.
4. Variation in parameter $P_{max}$: To investigate the effect of parameter $P_{max}$, TSA was simulate for 1, 2, 3, and 4 by keeping other parameters fixed. Table 11 and Fig. 9(d) show the effect of $P_{max}$ on various benchmark test functions. It is seen that TSA generates better optimal results when the value of $P_{max}$ is fixed to 4.

### 4.6. Scalability study

This subsection describes the effect of scalability on various test functions by using proposed TSA. The dimensionality of the test functions is made to vary as 30, 50, 80, and 100. Fig. 10 shows the performance of TSA algorithm on scalable benchmark test functions. It is observed that the performance of TSA is not too much degraded when the dimensionality of search space is increased. The results reveal that the performance of TSA is least affected with the increase in dimensionality of search space. This is due to better capability of the proposed TSA for balancing between exploration and exploitation.

### 4.7. Statistical testing

Apart from standard statistical analysis such as mean and standard deviation, Analysis of Variance (ANOVA) test has been conducted. ANOVA test is used to determine whether the results obtained from proposed algorithm are different from other competitor algorithms in a statistically significant way. The sample size for ANOVA test is 30 with 95% confidence of interval. A $p-$ value determine whether the given algorithm is statistically significant or not. If $p-$ value of the given algorithm is less than 0.05, then the corresponding algorithm is statistically significant. Table 12 shows the analysis of ANOVA test on the benchmark test functions. It is observed from Table 12 that the $p-$ value obtained from TSA is much smaller than 0.05 for all the benchmark test functions. Therefore, the proposed TSA is statistical different from the other competitor algorithms.

## 5. TSA for engineering design problems

TSA algorithm is tested on six constrained and one unconstrained engineering design problems. These problems are pressure vessel, speed reducer, welded beam, tension/compression spring, 25-bar truss, rolling element bearing, and displacement of loaded structure.

### 5.1. Constrained engineering design problems

This subsection describes six constrained engineering design problems to validate the performance of proposed algorithm.

#### 5.1.1. Pressure vessel design problem

This problem was first proposed by Kannan and Kramer (1994) to minimize the total cost of material, forming, and welding of a cylindrical vessel. The schematic view of pressure vessel design problem is shown in Fig. 11. There are four design variables:

- $T_s$ ($z_1$, thickness of the shell).
- $T_h$ ($z_2$, thickness of the head).
- $R$ ($z_3$, inner radius).
- $L$ ($z_4$, length of the cylindrical section without considering the head).

Apart from these, $R$ and $L$ are continuous variables whereas $T_s$ and $T_h$ are integer values which are multiples of 0.0625 in. The mathematical

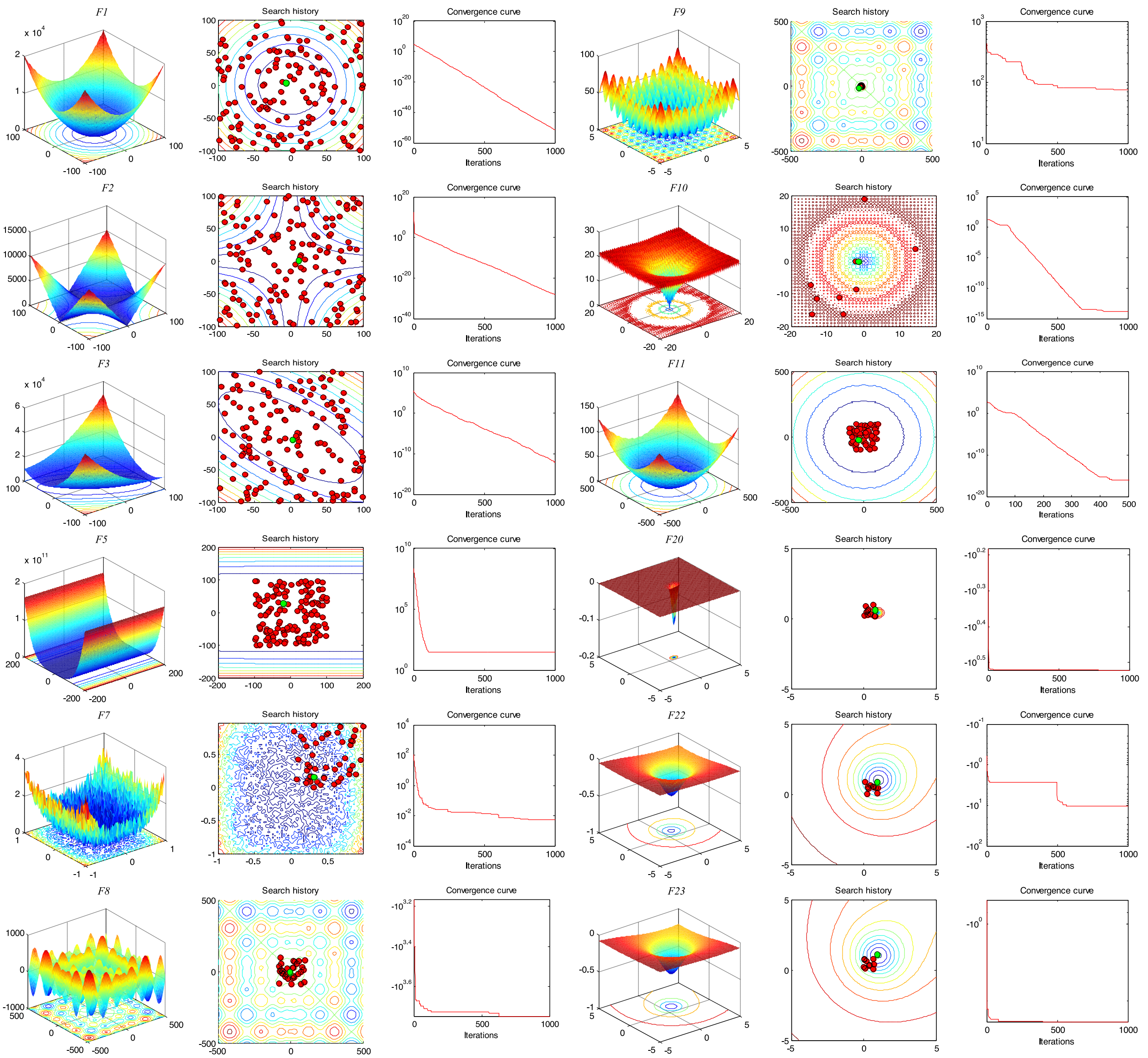


**Fig. 8.** Convergence analysis of the proposed TSA and search history on benchmark test problems.

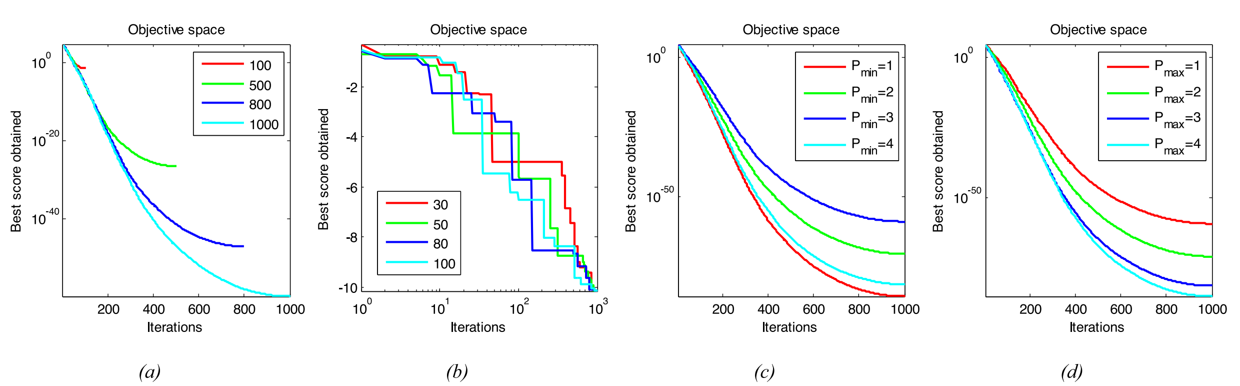


**Fig. 9.** Sensitivity analysis of the proposed TSA algorithm for, (a) Number of iterations; (b) Number of search agents; (c) Control parameter $P_{min}$; (d) Control parameter $P_{max}$.

**Table 8**
The obtained optimal values on unimodal, multimodal, fixed-dimension multimodal, composite, and CEC-2015 benchmark test functions using different simulation runs (i.e., 100, 500, 800, and 1000).

| Iterations | Functions | | | | | | |
|---|---|---|---|---|---|---|---|
| | $F_1$ | $F_5$ | $F_{11}$ | $F_{17}$ | $F_{23}$ | $F_{24}$ | $CEC-1$ |
| 100 | 8.19E−12 | 5.01E+02 | 7.29E−05 | 5.21E−03 | −2.42E+01 | 4.48E+04 | 1.29E+08 |
| 500 | 4.41E−19 | 5.07E+02 | 4.22E−07 | 8.90E−03 | −2.91E+02 | 4.16E+04 | 5.51E+07 |
| 800 | 3.07E−23 | 5.26E+02 | 5.11E−04 | 7.77E−08 | −3.10E+02 | 3.91E+04 | 4.00E+05 |
| **1000** | **5.10E−31** | **4.00E+00** | **2.19E−17** | **7.08E−12** | **−3.42E+00** | **9.75E+01** | **4.40E+02** |

**Table 9**
The obtained optimal values on unimodal, multimodal, fixed-dimension multimodal, composite, and CEC-2015 benchmark test functions where number of iterations is fixed as 1000. The number of search agents are varied from 30 to 100.

| Search agents | Functions | | | | | | |
|---|---|---|---|---|---|---|---|
| | $F_1$ | $F_5$ | $F_{11}$ | $F_{17}$ | $F_{23}$ | $F_{24}$ | $CEC-1$ |
| 30 | 5.51E−10 | 5.11E+00 | 5.11E−02 | 5.26E−02 | −2.51E+00 | 1.30E+02 | 2.66E+06 |
| 50 | 5.42E−15 | 5.11E+02 | 3.11E−02 | 9.10E−01 | −2.81E+00 | 4.20E+02 | 1.20E+05 |
| **80** | **7.27E−30** | **4.00E+00** | **3.20E−09** | **5.15E−04** | **−4.49E+00** | **4.12E+01** | **1.57E+03** |
| 100 | 5.91E−13 | 5.40E+00 | 8.10E−01 | 6.00E−02 | −3.12E+00 | 2.86E+03 | 2.75E+06 |

**Table 10**
The obtained optimal values on unimodal, multimodal, fixed-dimension multimodal, composite, and CEC-2015 benchmark test functions where number of iterations and search agents are fixed as 1000 and 80, respectively. The parameter $P_{min}$ is varied from [1, 2, 3, 4].

| $P_{min}$ | Functions | | | | | | |
|---|---|---|---|---|---|---|---|
| | $F_1$ | $F_5$ | $F_{11}$ | $F_{17}$ | $F_{23}$ | $F_{24}$ | $CEC-1$ |
| **1** | **1.10E−31** | **5.00E+00** | **4.45E−07** | **5.01E−03** | **−3.50E+00** | **1.01E+01** | **8.24E+03** |
| 2 | 9.93E−19 | 9.09E+01 | 8.88E−02 | 1.70E−00 | −2.11E+00 | 5.00E+03 | 9.59E+07 |
| 3 | 2.11E−12 | 5.60E+01 | 2.00E−01 | 8.01E−01 | −2.88E+00 | 4.45E+03 | 3.48E+07 |
| 4 | 1.52E−20 | 3.48E+01 | 8.17E−02 | 4.00E−01 | −3.16E+00 | 7.97E+03 | 4.17E+06 |

**Table 11**
The obtained optimal values on unimodal, multimodal, fixed-dimension multimodal, composite, and CEC-2015 benchmark test functions where number of iterations and search agents are fixed as 1000 and 80, respectively. The parameter $f$ is fixed as 1. The parameter $P_{max}$ is varied from [1, 2, 3, 4].

| $P_{max}$ | Functions | | | | | | |
|---|---|---|---|---|---|---|---|
| | $F_1$ | $F_5$ | $F_{11}$ | $F_{17}$ | $F_{23}$ | $F_{24}$ | $CEC-1$ |
| 1 | 5.46E−19 | 7.18E+01 | 4.41E−02 | 9.90E−00 | −2.22E+00 | 1.70E+03 | 2.40E+05 |
| 2 | 1.71E−20 | 2.36E+00 | 1.21E−03 | 7.56E−01 | −2.93E+00 | 3.17E+03 | 2.61E+04 |
| 3 | 8.15E−23 | 5.05E+00 | 7.90E−03 | 5.00E−01 | −3.07E+00 | 3.81E+03 | 1.00E+06 |
| **4** | **1.17E−28** | **1.00E+00** | **2.00E−09** | **2.47E−02** | **−3.51E+00** | **1.99E+01** | **4.05E+02** |

formulation of this problem is described below:

$$\text{Consider } \vec{z} = [z_1\ z_2\ z_3\ z_4] = [T_s\ T_h\ R\ L],$$

$$\text{Minimize } f(\vec{z}) = 0.6224 z_1 z_3 z_4 + 1.7781 z_2 z_3^2 + 3.1661 z_1^2 z_4 + 19.84 z_1^2 z_3,$$

Subject to:

$$g_1(\vec{z}) = -z_1 + 0.0193 z_3 \leq 0,$$

$$g_2(\vec{z}) = -z_3 + 0.00954 z_3 \leq 0,$$

$$g_3(\vec{z}) = -\pi z_3^2 z_4 - \frac{4}{3}\pi z_3^3 + 1{,}296{,}000 \leq 0,$$

$$g_4(\vec{z}) = z_4 - 240 \leq 0,$$

where,

$$1 \times 0.0625 \leq z_1,\ z_2 \leq 99 \times 0.0625,\ 10.0 \leq z_3,\ z_4 \leq 200.0. \tag{8}$$

Table 13 shows the comparison between TSA and other competitor algorithms such as EPO, SHO, GWO, PSO, MVO, SCA, GSA, and GA. TSA obtains optimal solution at point $z_{1-4} = (0.778090, 0.383230, 40.315050, 200.00000)$ and its fitness value is $f(z_{1-4}) = 5870.9550$. It can be clear from table that TSA algorithm is capable to find an optimal design with low cost.

The obtained statistical results of this problem are given in Table 14. It can be analyzed from table that TSA achieves optimal values in terms of best, mean, and median as compared to other algorithms. The convergence analysis of TSA on this problem for best optimal design is shown in Fig. 12.

#### 5.1.2. Speed reducer design problem

The speed reducer design problem is an engineering design problem. It has seven design variables (Gandomi and Yang, 2011) as shown in Fig. 13. The main objective of this design problem is to minimize the weight of speed reducer with subject to the following constraints (Mezura-Montes and Coello, 2005):

- Bending stress of the gear teeth.
- Surface stress.
- Transverse deflections of the shafts.
- Stresses in the shafts.

There are seven design variables ($z_1 - z_7$) such as face width ($b$), module of teeth ($m$), number of teeth in the pinion ($p$), length of the first shaft between bearings ($l_1$), length of the second shaft between bearings ($l_2$), diameter of first ($d_1$) shafts, and diameter of second shafts ($d_2$). The

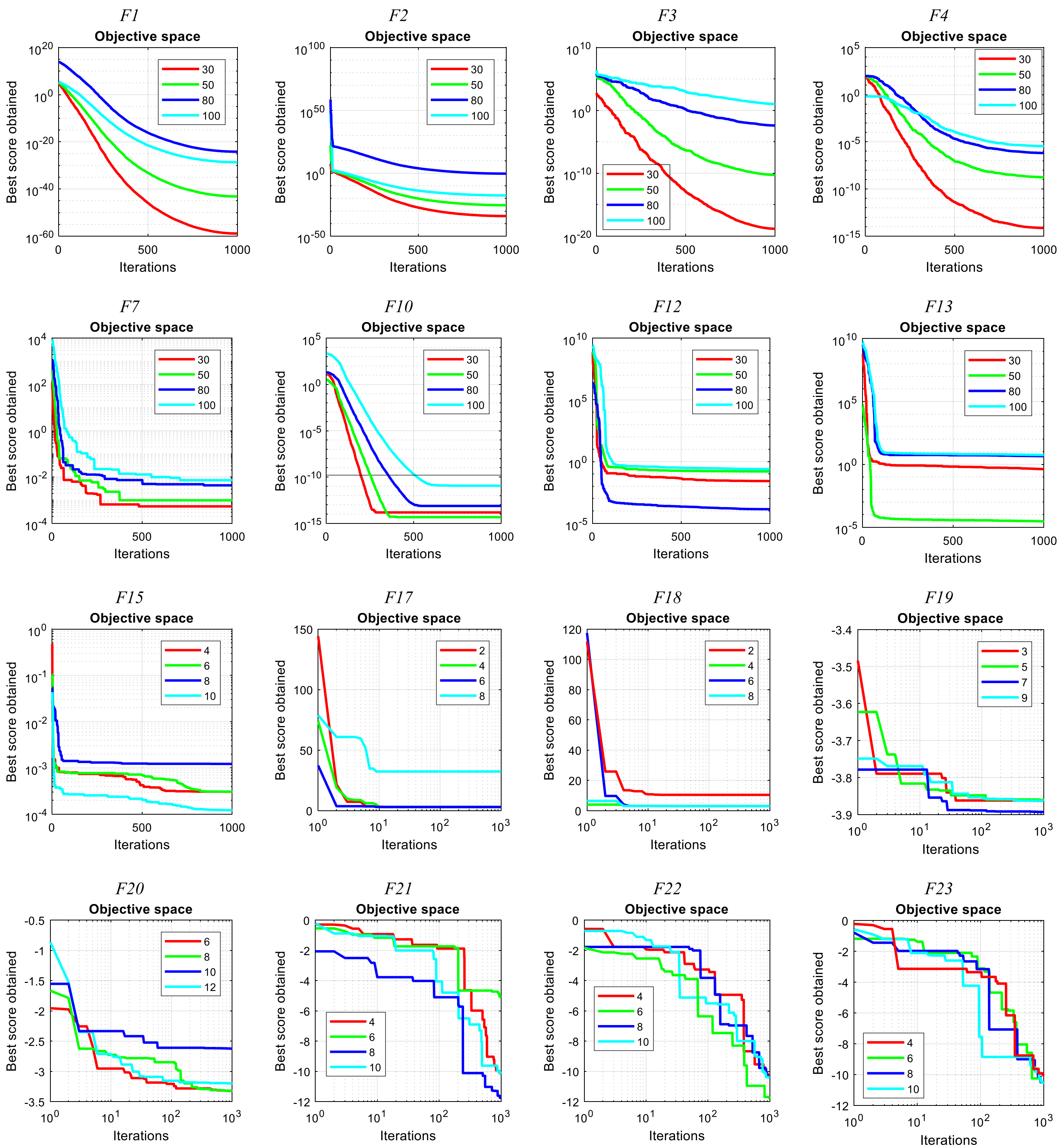


**Fig. 10.** Effect of scalability on the performance of TSA algorithm.

mathematical formulation of this problem is described as follows:

$$
\begin{aligned}
&\text{Consider } \vec{z} = [z_1\ z_2\ z_3\ z_4\ z_5\ z_6\ z_7] = [b\ m\ p\ l_1\ l_2\ d_1\ d_2],\\
&\text{Minimize } f(\vec{z}) = 0.7854 z_1 z_2^2 (3.3333 z_3^2 + 14.9334 z_3 - 43.0934)\\
&\ - 1.508 z_1 (z_6^2 + z_7^2) + 7.4777 (z_6^3 + z_7^3) + 0.7854 (z_4 z_6^2 + z_5 z_7^2),\\
&\text{Subject to:}\\
&g_1(\vec{z}) = \frac{27}{z_1 z_2^2 z_3} - 1 \le 0,\\
&g_2(\vec{z}) = \frac{397.5}{z_1 z_2^2 z_3^2} - 1 \le 0,\\
&g_3(\vec{z}) = \frac{1.93 z_4^3}{z_2 z_6^4 z_3} - 1 \le 0,\\
&g_4(\vec{z}) = \frac{1.93 z_5^3}{z_2 z_7^4 z_3} - 1 \le 0,\\
&g_5(\vec{z}) = \frac{[(745(z_4/z_2 z_3))^2 + 16.9 \times 10^6]^{1/2}}{110 z_6^3} - 1 \le 0,\\
&g_6(\vec{z}) = \frac{[(745(z_5/z_2 z_3))^2 + 157.5 \times 10^6]^{1/2}}{85 z_7^3} - 1 \le 0,
\end{aligned}
\tag{9}
$$

**Table 12**
Analysis of Variance (ANOVA) test results.

| $F$ | $p-$ value | TSA | SHO | GWO | PSO | MVO | SCA | GSA | GA | EPO |
|---|---|---|---|---|---|---|---|---|---|---|
| $F_1$ | 4.70E−11 | SHO, GWO, PSO, SCA, GSA, GA, EPO | TSA, GWO, PSO, MVO, SCA, GSA, GA, EPO | TSA, SHO, PSO, SCA, GSA, GA, EPO | TSA, SHO, GWO, MVO, SCA, GSA, GA, EPO | TSA, SHO, PSO, SCA, GA, EPO | TSA, SHO, GWO, GSA, GA, EPO | TSA, SHO, GWO, PSO, MVO, SCA, GA, EPO | TSA, SHO, GWO, MVO, SCA, GSA, EPO | TSA, SHO, GWO, MVO, SCA, GSA, GA |
| $F_2$ | 6.66E−20 | SHO, GWO, PSO, MVO, SCA, GA, EPO | TSA, GWO, PSO, MVO, SCA, GSA, GA, EPO | TSA, SHO, PSO, SCA, GSA, GA, EPO | TSA, GWO, MVO, SCA, GSA, GA, EPO | TSA, GWO, PSO, SCA, GSA, GA | TSA, SHO, PSO, GSA, GA, EPO | TSA, SHO, GWO, PSO, MVO, SCA, GA, EPO | TSA, SHO, GWO, PSO, SCA, EPO | TSA, SHO, GWO, PSO, MVO, SCA, GSA |
| $F_3$ | 1.50E−46 | SHO, GWO, PSO, SCA, GSA, GA, EPO | TSA, GWO, PSO, SCA, GSA, GA | TSA, SHO, MVO, SCA, GSA, GA, EPO | TSA, SHO, GWO, MVO, SCA, GSA, GA, EPO | TSA, GWO, PSO, SCA, GSA, GA, EPO | TSA, SHO, MVO, GA, EPO | TSA, SHO, GWO, PSO, MVO, SCA, EPO | TSA, SHO, GWO, PSO, MVO, SCA, GSA, EPO | TSA, SHO, PSO, MVO, SCA, GA |
| $F_4$ | 8.82E−80 | SHO, GWO, PSO, MVO, SCA, GSA, GA, EPO | TSA, GWO, PSO, MVO, SCA, GSA, GA, EPO | TSA, SHO, PSO, MVO, SCA, GSA, GA, EPO | TSA, SHO, GWO, SCA, GSA, GA, EPO | TSA, SHO, GWO, SCA, GSA, GA, EPO | TSA, SHO, GWO, GSA, GA, EPO | TSA, SHO, GWO, PSO, MVO, SCA, GA, EPO | TSA, SHO, GWO, PSO, MVO, SCA, GSA, EPO | TSA, SHO, GWO, MVO, SCA, GSA, GA |
| $F_5$ | 2.88E−11 | SHO, GWO, PSO, MVO, SCA, GSA, GA, EPO | TSA, PSO, MVO, SCA, GSA, GA, EPO | TSA, SHO, PSO, MVO, SCA, GSA, GA, EPO | TSA, SHO, GWO, MVO, SCA, GSA, GA, EPO | TSA, SHO, GWO, SCA, GSA | TSA, SHO, GWO, PSO, GSA, GA, EPO | TSA, SHO, GWO, PSO, MVO, SCA, GA, EPO | TSA, GWO, PSO, MVO, SCA, GSA, EPO | TSA, SHO, GWO, PSO, MVO GSA, GA |
| $F_6$ | 9.70E−17 | SHO, GWO, PSO, MVO, SCA, GSA, GA, EPO | TSA, GWO, PSO, MVO, SCA, GA, EPO | TSA, SHO, PSO, MVO, SCA, GSA, GA, EPO | TSA, SHO, MVO, SCA, GSA, GA, EPO | TSA, SHO, PSO, GSA, GA, EPO | TSA, SHO, MVO, GSA, GA, EPO | TSA, SHO, PSO, SCA, GA, EPO | TSA, SHO, PSO, SCA, GSA, EPO | TSA, SHO, GWO, PSO, MVO, GSA, GA |
| $F_7$ | 6.16E−65 | SHO, GWO, PSO, MVO, SCA, GSA | TSA, GWO, PSO, MVO, SCA, GSA, GA, EPO | TSA, SHO, PSO, MVO, SCA, GA, EPO | TSA, SHO, MVO, SCA, GSA, GA, EPO | TSA, SHO, PSO, SCA, GSA, GA, EPO | TSA, SHO, GWO, MVO, GSA | TSA, SHO, GWO, PSO, MVO, SCA, GA, EPO | TSA, SHO, GWO, PSO, MVO, SCA, GSA | TSA, SHO, GWO, PSO, SCA, GSA, GA |
| $F_8$ | 3.53E−11 | SHO, GWO, MVO, SCA, GA, EPO | TSA, GWO, MVO, SCA, GSA, EPO | TSA, SHO, PSO, MVO, SCA, GA, EPO | TSA, SHO, MVO, SCA, GSA, GA | TSA, SHO, PSO, GSA, GA, EPO | TSA, SHO, GWO, PSO, GSA, EPO | TSA, SHO, PSO, SCA, GA, EPO | TSA, SHO, GWO, MVO, SCA, GSA, EPO | TSA, SHO, PSO, MVO, SCA |
| $F_9$ | 2.31E−24 | SHO, GWO, PSO, MVO, SCA, GSA, GA, EPO | TSA, GWO, MVO, GSA, GA, EPO | TSA, SHO, PSO, MVO, SCA, GSA, GA, EPO | TSA, SHO, SCA, GSA, GA, EPO | TSA, SHO, PSO, SCA, GSA, GA, EPO | TSA, SHO, PSO, GSA, GA, EPO | TSA, SHO, PSO, MVO, GA, EPO | TSA, SHO, GWO, PSO, MVO, SCA, GSA, EPO | TSA, SHO, GWO, PSO, SCA, GSA, GA |
| $F_{10}$ | 6.11E−66 | SHO, GWO, PSO, MVO, SCA, GSA, GA, EPO | TSA, GWO, PSO, SCA, GSA, GA, EPO | TSA, SHO, PSO, MVO, SCA, GSA, GA, EPO | TSA, SHO, GWO, GSA | TSA, GWO, PSO, SCA, GSA, GA, EPO | TSA, SHO, GWO, MVO, GA, EPO | TSA, GWO, PSO, MVO, SCA, GA, EPO | TSA, SHO, GWO, SCA | TSA, SHO, GWO, PSO, MVO, SCA, GSA, GA |
| $F_{11}$ | 5.21E−97 | SHO, GWO, PSO, MVO, SCA, GSA, EPO | TSA, GWO, PSO, MVO, SCA, GSA, GA, EPO | TSA, SHO, MVO, SCA, GSA, GA, EPO | TSA, SHO, GWO, MVO, SCA, GSA, GA, EPO | TSA, SHO, PSO, GSA, GA, EPO | TSA, SHO, GWO, PSO, MVO, GSA, EPO | TSA, SHO, GWO, MVO, SCA, GA, EPO | TSA, SHO, GWO, PSO, MVO, SCA, EPO | TSA, SHO, GWO, PSO, MVO, GSA, GA |
| $F_{12}$ | 3.98E−71 | SHO, GWO, PSO, MVO, SCA, GSA, GA, EPO | TSA, GWO, PSO, SCA, GSA, GA, EPO | TSA, SHO, MVO, SCA, GSA, GA, EPO | TSA, SHO, GWO, MVO, GSA, GA, EPO | TSA, SHO, GWO, SCA, GSA, GA, EPO | TSA, SHO, GWO, GSA, GA, EPO | TSA, SHO, GWO, MVO, SCA, GA, EPO | TSA, SHO, PSO, MVO, SCA, GSA, EPO | TSA, SHO, GWO, PSO, MVO, SCA, GA |
| $F_{13}$ | 3.60E−16 | SHO, GWO, PSO, MVO, SCA, GSA, GA, EPO | TSA, GWO, PSO, MVO, SCA, GA, EPO | TSA, SHO, PSO, MVO, SCA, GSA, GA, EPO | TSA, SHO, SCA, GSA, GA, EPO | TSA, SHO, PSO, SCA, GSA, GA, EPO | TSA, SHO, GWO, PSO, GSA, GA, EPO | TSA, SHO, GWO, PSO, MVO, SCA, GA, EPO | TSA, SHO, PSO, MVO, GSA, EPO | TSA, SHO, PSO, MVO, SCA, GA |
| $F_{14}$ | 5.24E−57 | SHO, GWO, PSO, MVO, SCA, GSA, EPO | TSA, GWO, PSO, MVO, SCA, GSA, GA, EPO | TSA, SHO, PSO, SCA, GSA | TSA, SHO, MVO, SCA, GSA, GA, EPO | TSA, SHO, PSO, GSA, GA, EPO | TSA, SHO, GWO, GSA, GA, EPO | TSA, GWO, PSO, SCA, GA, EPO | TSA, SHO, GWO, PSO, MVO, GSA, EPO | TSA, SHO, GWO, MVO, SCA |
| $F_{15}$ | 4.19E−17 | SHO, GWO, PSO, MVO, SCA, GSA, GA, EPO | TSA, GWO, PSO, MVO, GSA, EPO | TSA, SHO, PSO, SCA, GSA, GA, EPO | TSA, SHO, MVO, SCA, GSA, GA, EPO | TSA, SHO, GWO, SCA, GSA | TSA, SHO, GWO, PSO, MVO, GA, EPO | TSA, SHO, PSO, SCA, GA, EPO | TSA, SHO, GWO, MVO, SCA, GSA | TSA, SHO, GWO, PSO, MVO |
| $F_{16}$ | 4.21E−46 | SHO, GWO, PSO, MVO, SCA, GSA, GA, EPO | TSA, GWO, MVO, GSA, GA, EPO | TSA, SHO, PSO, MVO, SCA, GSA, GA, EPO | TSA, SHO, GWO, MVO, SCA, GSA, GA, EPO | TSA, GWO, PSO, SCA, GSA, GA, EPO | TSA, SHO, GWO, GSA | TSA, SHO, GWO, PSO, MVO, SCA | TSA, SHO, GWO, MVO, SCA, GSA, EPO | TSA, SHO, GWO, MVO, SCA, GA |
| $F_{17}$ | 1.11E−59 | SHO, GWO, PSO, MVO, SCA, GSA, GA, EPO | TSA, GWO, PSO, MVO, SCA, GSA, GA, EPO | TSA, SHO, PSO, MVO, GSA, GA, EPO | TSA, SHO, GWO, SCA, GSA, GA, EPO | TSA, SHO, PSO, SCA, GA, EPO | TSA, SHO, PSO, GSA, GA, EPO | TSA, SHO, GWO, SCA, GA, EPO | TSA, SHO, GWO, MVO, SCA, GSA, EPO | TSA, SHO, GWO, MVO, SCA, GSA, GA |

(*continued on next page*)

**Table 12** (*continued*).

| $F$ | $p-$ value | TSA | SHO | GWO | PSO | MVO | SCA | GSA | GA | EPO |
|---|---|---|---|---|---|---|---|---|---|---|
| $F_{18}$ | 7.35E−06 | SHO, GWO, PSO, MVO, GSA, GA, EPO | TSA, GWO, PSO, MVO, SCA, GA, EPO | TSA, SHO, MVO, SCA, GSA, GA, EPO | TSA, SHO, GSA, GA | TSA, SHO, PSO, SCA, GSA, EPO | TSA, SHO, GWO, PSO, GSA, GA, EPO | TSA, SHO, GWO, PSO, MVO | TSA, SHO, PSO, MVO, SCA, EPO | TSA, SHO, GWO, PSO, MVO, SCA, GSA, GA |
| $F_{19}$ | 5.41E−52 | SHO, GWO, PSO, MVO, SCA, GSA, GA, EPO | TSA, GWO, PSO, SCA, GSA, GA, EPO | TSA, SHO, PSO, MVO, SCA, GA, EPO | TSA, SHO, GWO, SCA, GSA, GA, EPO | TSA, SHO, PSO, SCA, GA, EPO | TSA, SHO, PSO, MVO, GA, EPO | TSA, SHO, GWO, PSO, MVO, SCA, EPO | TSA, SHO, PSO, SCA | TSA, GWO, PSO, MVO, SCA, GSA, GA |
| $F_{20}$ | 6.50E−11 | SHO, GWO, PSO, MVO, SCA, GSA | TSA, GWO, PSO, MVO, SCA, GSA | TSA, PSO, MVO, SCA, GSA, | TSA, SHO, GWO, MVO, SCA, GSA, GA, EPO | TSA, SHO, GWO, PSO, SCA, GSA, GA, EPO | TSA, SHO, PSO, GSA | TSA, SHO, GWO, MVO, SCA, GA, EPO | TSA, SHO, PSO, MVO, GSA, EPO | TSA, SHO, GWO, PSO, MVO, SCA, GSA, GA |
| $F_{21}$ | 5.10E−03 | SHO, GWO, PSO, MVO, SCA, GSA, GA, EPO | TSA, GWO, PSO, MVO, GSA, GA, EPO | TSA, SHO, PSO, MVO, GSA, GA, EPO | TSA, SHO, GWO, MVO, SCA | TSA, SHO, GWO, PSO, SCA, GSA, GA, EPO | TSA, SHO, GWO, PSO, MVO, GSA, GA, EPO | TSA, SHO, PSO, SCA | TSA, SHO, GWO, PSO, MVO, SCA, GSA, EPO | TSA, SHO, GWO, PSO, MVO, SCA, GSA, GA |
| $F_{22}$ | 2.10E−25 | SHO, GWO, PSO, MVO, SCA, GSA, GA, EPO | TSA, GWO, PSO, MVO, GSA, GA, EPO | TSA, SHO, PSO, MVO, SCA, GSA, GA, EPO | TSA, MVO, SCA, GA, EPO | TSA, SHO, GWO, PSO, SCA, GSA, GA, EPO | TSA, SHO, PSO, GSA, GA, EPO | TSA, SHO, GWO, PSO, MVO, SCA, GA, EPO | TSA, GWO, PSO, SCA, GSA, EPO | TSA, SHO, PSO, MVO, SCA, GSA, GA |
| $F_{23}$ | 3.75E−42 | SHO, GWO, PSO, MVO, SCA, GSA, GA, EPO | TSA, GWO, MVO, SCA, GSA, EPO | TSA, SHO, PSO, MVO, SCA, GSA, GA, EPO | TSA, SHO, GWO, MVO, SCA, GSA, GA, EPO | TSA, SHO, PSO, GSA, GA, EPO | TSA, SHO, GWO, PSO, MVO, GSA, GA | TSA, SHO, MVO, SCA, GA, EPO | TSA, SHO, GWO, MVO, SCA, GSA | TSA, SHO, GWO, PSO, MVO, SCA, GSA, GA |
| $F_{24}$ | 1.52E−43 | SHO, GWO, PSO, MVO, SCA, GSA, GA, EPO | TSA, GWO, PSO, MVO, SCA, GSA, GA | TSA, SHO, MVO, GSA, GA, EPO | GWO, MVO, SCA, GSA, GA, EPO | TSA, GWO, PSO, SCA, GSA, GA | TSA, SHO, GWO, PSO, GSA, GA, EPO | SHO, GWO, PSO, MVO, SCA, EPO | TSA, SHO, PSO, MVO, SCA, GSA, EPO | TSA, SHO, GWO, PSO, MVO, SCA, GSA, GA |
| $F_{25}$ | 3.01E−02 | SHO, GWO, PSO, MVO, SCA, GSA, GA, EPO | TSA, GWO, MVO, SCA, GSA, GA | TSA, SHO, PSO, MVO, SCA, GA, EPO | TSA, SHO, GWO, MVO, SCA, GSA, EPO | TSA, GWO, SCA, GSA, EPO | TSA, SHO, GWO, PSO, GSA, GA, EPO | TSA, SHO, GWO, PSO, MVO, SCA | TSA, SHO, PSO, SCA, GSA, EPO | TSA, SHO, PSO, SCA, GSA, GA |
| $F_{26}$ | 4.78E−30 | SHO, GWO, PSO, MVO, SCA, GSA, GA | TSA, PSO, SCA, GSA, GA, EPO | TSA, SHO, PSO, MVO, SCA | TSA, SHO, MVO, SCA, GSA, GA, EPO | TSA, SHO, GWO, PSO, SCA, GSA, GA, EPO | TSA, SHO, GWO, PSO, MVO, GSA, GA, EPO | TSA, PSO, GA, EPO | TSA, SHO, GWO, PSO, MVO, SCA, GSA, EPO | TSA, SHO, GWO, PSO, MVO, SCA, GSA |
| $F_{27}$ | 9.15E−02 | SHO, GWO, PSO, MVO, SCA, GSA, GA, EPO | TSA, GWO, PSO, MVO, SCA, GA, EPO | TSA, SHO, PSO, MVO, SCA, GSA, GA, EPO | TSA, GWO, MVO, GSA, GA, EPO | TSA, SHO, PSO, SCA, GSA, GA, EPO | TSA, SHO, MVO, GSA, GA, EPO | TSA, SHO, GWO, PSO, SCA, GA, EPO | TSA, SHO, GWO, MVO, SCA, GSA, EPO | TSA, SHO, GWO, PSO, MVO, SCA, GSA |
| $F_{28}$ | 2.31E−92 | SHO, GWO, PSO, MVO, SCA, GSA, EPO | TSA, MVO, GSA, GA, EPO | TSA, PSO, MVO, SCA, GSA, EPO | TSA, SHO, GWO, MVO, GSA, GA, EPO | TSA, SHO, PSO, GSA, GA, EPO | TSA, GWO, PSO, MVO, GA | TSA, GWO, PSO, MVO, SCA, GA, EPO | TSA, SHO, GWO, MVO, SCA, GSA, EPO | TSA, SHO, GWO, PSO, MVO, SCA, GSA, GA |
| $F_{29}$ | 4.16E−06 | SHO, GWO, MVO, SCA, GSA, GA, EPO | TSA, GWO, PSO, MVO, SCA, GSA, GA, EPO | TSA, SHO, MVO, GSA | TSA, SHO, GWO, MVO, SCA, GSA, GA, EPO | TSA, SHO, GWO, PSO, SCA, GSA, GA, EPO | TSA, SHO, MVO, GSA, GA, EPO | TSA, SHO, GWO, PSO, MVO, SCA, GA, EPO | TSA, SHO, PSO, MVO, SCA, GSA | TSA, SHO, PSO, MVO, GSA, GA |

**Table 13**
Comparison of best solution obtained from different algorithms for pressure vessel design problem.

| Algorithms | Optimum variables | | | | Optimum cost |
|---|---|---|---|---|---|
| | $T_s$ | $T_h$ | $R$ | $L$ | |
| TSA | 0.778090 | 0.383230 | 40.315050 | 200.00000 | **5870.9550** |
| EPO | 0.778099 | 0.383241 | 40.315121 | 200.00000 | 5880.0700 |
| SHO | 0.778210 | 0.384889 | 40.315040 | 200.00000 | 5885.5773 |
| GWO | 0.779035 | 0.384660 | 40.327793 | 199.65029 | 5889.3689 |
| PSO | 0.778961 | 0.384683 | 40.320913 | 200.00000 | 5891.3879 |
| MVO | 0.845719 | 0.418564 | 43.816270 | 156.38164 | 6011.5148 |
| SCA | 0.817577 | 0.417932 | 41.74939 | 183.57270 | 6137.3724 |
| GSA | 1.085800 | 0.949614 | 49.345231 | 169.48741 | 11 550.2976 |
| GA | 0.752362 | 0.399540 | 40.452514 | 198.00268 | 5890.3279 |

$$g_7(\vec{z}) = \frac{z_2 z_3}{40} - 1 \leq 0,$$
$$g_8(\vec{z}) = \frac{5z_2}{z_1} - 1 \leq 0,$$
$$g_9(\vec{z}) = \frac{z_1}{12z_2} - 1 \leq 0,$$

**Table 14**
Statistical results obtained from different algorithms for pressure vessel design problem.

| Algorithms | Best | Mean | Worst | Std. Dev. | Median |
|---|---|---|---|---|---|
| TSA | **5870.9550** | **5880.5240** | 5882.6580 | 009.125 | **5875.9685** |
| EPO | 5880.0700 | 5884.1401 | 5891.3099 | 024.341 | 5883.5153 |
| SHO | 5885.5773 | 5887.4441 | 5892.3207 | **002.893** | 5886.2282 |
| GWO | 5889.3689 | 5891.5247 | 5894.6238 | 013.910 | 5890.6497 |
| PSO | 5891.3879 | 6531.5032 | 7394.5879 | 534.119 | 6416.1138 |
| MVO | 6011.5148 | 6477.3050 | 7250.9170 | 327.007 | 6397.4805 |
| SCA | 6137.3724 | 6326.7606 | 6512.3541 | 126.609 | 6318.3179 |
| GSA | 11 550.2976 | 23 342.2909 | **33 226.2526** | 5790.625 | 24 010.0415 |
| GA | 5890.3279 | 6264.0053 | 7005.7500 | 496.128 | 6112.6899 |

$$g_{10}(\vec{z}) = \frac{1.5z_6 + 1.9}{z_4} - 1 \leq 0,$$
$$g_{11}(\vec{z}) = \frac{1.1z_7 + 1.9}{z_5} - 1 \leq 0,$$

where,

$$2.6 \leq z_1 \leq 3.6,\ 0.7 \leq z_2 \leq 0.8,\ 17 \leq z_3 \leq 28,\ 7.3 \leq z_4 \leq 8.3,$$
$$7.3 \leq z_5 \leq 8.3,\ 2.9 \leq z_6 \leq 3.9,\ 5.0 \leq z_7 \leq 5.5.$$

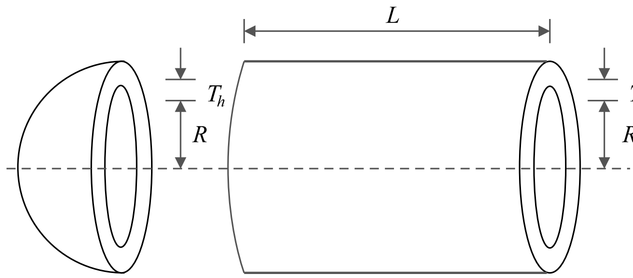


**Fig. 11.** Schematic view of pressure vessel design problem.

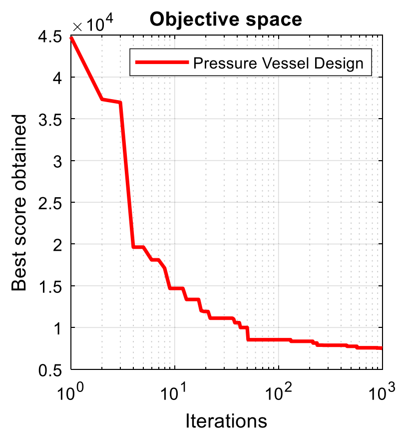


**Fig. 12.** Convergence analysis of TSA for pressure vessel design problem.

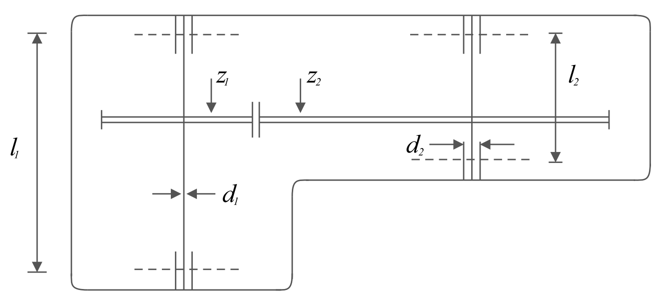


**Fig. 13.** Schematic view of speed reducer design problem.

Table 15 reveals the obtained optimal solutions by different algorithms on this design problem. The proposed TSA algorithm obtains optimal solution at point $z_{1-7} = (3.50120, 0.7, 17, 7.3, 7.8, 3.33410, 5.26530)$ with corresponding fitness value as $f(z_{1-7}) = 2990.9580$. The statistical results of TSA and other optimization algorithms are tabulated in Table 16.

The results show that TSA is superior than other metaheuristic optimization algorithms. Fig. 14 shows the convergence behavior of the proposed TSA on speed reducer design problem.

### 5.1.3. Welded beam design problem

The objective of this optimization problem is to minimize the fabrication cost of welded beam as shown in Fig. 15. The optimization constraints of welded beam are shear stress ($\tau$), bending stress ($\theta$) in the beam, buckling load ($P_c$) on the bar, and end deflection ($\delta$) of the beam. There are four design variables ($z_1 - z_4$) of this problem which are described as:

- $h$ ($z_1$, thickness of weld)
- $l$ ($z_2$, length of the clamped bar)
- $t$ ($z_3$, height of the bar)

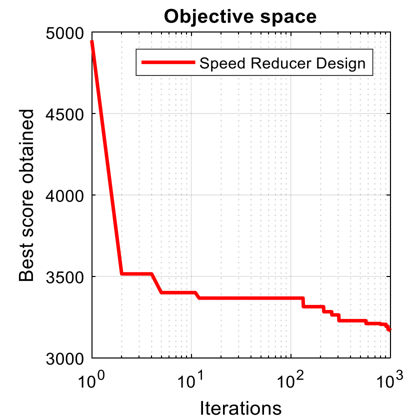


**Fig. 14.** Convergence analysis of the proposed TSA algorithm for speed reducer design problem.

- $b$ ($z_4$, thickness of the bar)

The mathematical formulation is described as follows:

$$\begin{aligned}
&\text{Consider } \vec{z} = [z_1\ z_2\ z_3\ z_4] = [h\ l\ t\ b],\\
&\text{Minimize } f(\vec{z}) = 1.10471 z_1^2 z_2 + 0.04811 z_3 z_4 (14.0 + z_2),\\
&\text{Subject to:}\\
&g_1(\vec{z}) = \tau(\vec{z}) - 13{,}600 \le 0,\\
&g_2(\vec{z}) = \sigma(\vec{z}) - 30{,}000 \le 0,\\
&g_3(\vec{z}) = \delta(\vec{z}) - 0.25 \le 0,\\
&g_4(\vec{z}) = z_1 - z_4 \le 0,\\
&g_5(\vec{z}) = 6000 - P_c(\vec{z}) \le 0,\\
&g_6(\vec{z}) = 0.125 - z_1 \le 0,\\
&g_7(\vec{z}) = 1.10471 z_1^2 + 0.04811 z_3 z_4 (14.0 + z_2) - 5.0 \le 0,
\end{aligned} \tag{10}$$

where,

$$0.1 \le z_1,\ 0.1 \le z_2,\ z_3 \le 10.0,\ z_4 \le 2.0,$$

$$\tau(\vec{z}) = \sqrt{(\tau')^2 + (\tau'')^2 + (l\tau'\tau'')/\sqrt{0.25(l^2 + (h+t)^2)}},$$

$$\tau' = \frac{6000}{\sqrt{2}hl}, \qquad \sigma(\vec{z}) = \frac{504{,}000}{t^2 b}, \qquad \delta(\vec{z}) = \frac{65{,}856{,}000}{(30 \times 10^6) b t^3},$$

$$\tau'' = \frac{6000(14 + 0.5l)\sqrt{0.25(l^2 + (h+t)^2)}}{2[0.707hl(l^2/12 + 0.25(h+t)^2)]},$$

$$P_c(\vec{z}) = 64{,}746.022(1 - 0.0282346t)tb^3.$$

The comparison results between proposed TSA and other metaheuristics is given in Table 17. The proposed TSA obtains optimal solution at point $z_{1-4} = (0.203290, 3.471140, 9.035100, 0.201150)$ with corresponding fitness value equal to $f(z_{1-4}) = 1.721020$. Table 18 shows the statistical comparison of TSA and other competitor algorithms. TSA reveals the superiority than other algorithms in terms of best, mean, and median.

Fig. 16 shows the convergence behavior of best optimal solution obtained from the proposed TSA for welded beam design problem.

### 5.1.4. Tension/compression spring design problem

The objective of this engineering design problem is to minimize the tension/compression spring weight (see Fig. 17). The constraints are described as follows:

- Shear stress.
- Surge frequency.
- Minimum deflection.

There are three design variables: wire diameter ($d$), mean coil diameter ($D$), and the number of active coils ($P$). The mathematical

**Table 15**
Comparison of best solution obtained from different algorithms for speed reducer design problem.

| Algorithms | Optimum variables | | | | | | | Optimum cost |
|---|---|---|---|---|---|---|---|---|
| | $b$ | $m$ | $p$ | $l_1$ | $l_2$ | $d_1$ | $d_2$ | |
| TSA | 3.50120 | 0.7 | 17 | 7.3 | 7.8 | 3.33410 | 5.26530 | **2990.9580** |
| EPO | 3.50123 | 0.7 | 17 | 7.3 | 7.8 | 3.33421 | 5.26536 | 2994.2472 |
| SHO | 3.50159 | 0.7 | 17 | 7.3 | 7.8 | 3.35127 | 5.28874 | 2998.5507 |
| GWO | 3.506690 | 0.7 | 17 | 7.380933 | 7.815726 | 3.357847 | 5.286768 | 3001.288 |
| PSO | 3.500019 | 0.7 | 17 | 8.3 | 7.8 | 3.352412 | 5.286715 | 3005.763 |
| MVO | 3.508502 | 0.7 | 17 | 7.392843 | 7.816034 | 3.358073 | 5.286777 | 3002.928 |
| SCA | 3.508755 | 0.7 | 17 | 7.3 | 7.8 | 3.461020 | 5.289213 | 3030.563 |
| GSA | 3.600000 | 0.7 | 17 | 8.3 | 7.8 | 3.369658 | 5.289224 | 3051.120 |
| GA | 3.510253 | 0.7 | 17 | 8.35 | 7.8 | 3.362201 | 5.287723 | 3067.561 |

**Table 16**
Statistical results obtained from different algorithms for speed reducer design problem.

| Algorithms | Best | Mean | Worst | Std. Dev. | Median |
|---|---|---|---|---|---|
| TSA | **2990.9580** | **2993.010** | 2998.425 | **1.22408** | **2992.018** |
| EPO | 2994.2472 | 2997.482 | 2999.092 | 1.78091 | 2996.318 |
| SHO | 2998.5507 | 2999.640 | 3003.889 | 1.93193 | 2999.187 |
| GWO | 3001.288 | 3005.845 | 3008.752 | 5.83794 | 3004.519 |
| PSO | 3005.763 | 3105.252 | 3211.174 | 79.6381 | 3105.252 |
| MVO | 3002.928 | 3028.841 | 3060.958 | 13.0186 | 3027.031 |
| SCA | 3030.563 | 3065.917 | 3104.779 | 18.0742 | 3065.609 |
| GSA | 3051.120 | 3170.334 | **3363.873** | 92.5726 | 3156.752 |
| GA | 3067.561 | 3186.523 | 3313.199 | 17.1186 | 3198.187 |

formulation of this problem is described below:

Consider $\vec{z} = [z_1\ z_2\ z_3] = [d\ D\ P]$,

$$\text{Minimize } f(\vec{z}) = (z_3 + 2)z_2 z_1^2, \tag{11}$$

Subject to:

$$g_1(\vec{z}) = 1 - \frac{z_2^3 z_3}{71785 z_1^4} \le 0,$$

$$g_2(\vec{z}) = \frac{4z_2^2 - z_1 z_2}{12566(z_2 z_1^3 - z_1^4)} + \frac{1}{5108 z_1^2} \le 0,$$

$$g_3(\vec{z}) = 1 - \frac{140.45 z_1}{z_2^2 z_3} \le 0,$$

$$g_4(\vec{z}) = \frac{z_1 + z_2}{1.5} - 1 \le 0,$$

where,

$0.05 \le z_1 \le 2.0,\ 0.25 \le z_2 \le 1.3,\ 2.0 \le z_3 \le 15.0.$

Table 19 shows the comparison between proposed TSA and other competitor algorithms in terms of design variables values and objective values. TSA generated best solution at design variables $z_{1-3}$ = (0.051080, 0.342890, 12.0890) with an objective function value of $f(z_{1-3})$ = 0.012655520. The results show that TSA is better than the other competitor algorithms on this design problem. The statistical results of tension/compression spring design problem for the reported algorithms are also compared and given in Table 20. It is analyzed from Table 20 that TSA provides better statistical results in terms of best, mean, and median.

Fig. 18 shows the convergence analysis for best optimal design obtained from the proposed TSA.

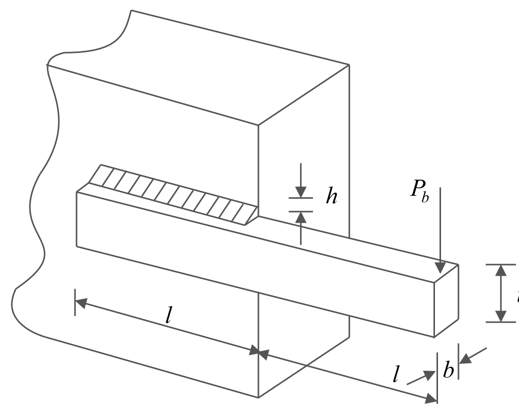


**Fig. 15.** Schematic view of welded beam problem.

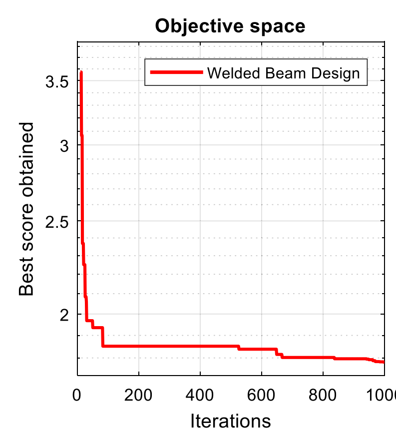


**Fig. 16.** Convergence analysis of TSA for welded beam design problem.

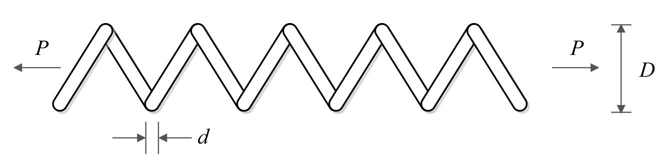


**Fig. 17.** Schematic view of tension/compression spring problem.

### 5.1.5. 25-bar truss design problem

The truss design problem is a popular large-scale optimization problem (Kaveh and Talatahari, 2009a,b) (see Fig. 19). There are 10 nodes and 25 bars cross-sectional members. These are grouped into eight categories.

- Group 1: $A_1$
- Group 2: $A_2, A_3, A_4, A_5$
- Group 3: $A_6, A_7, A_8, A_9$
- Group 4: $A_{10}, A_{11}$
- Group 5: $A_{12}, A_{13}$
- Group 6: $A_{14}, A_{15}, A_{17}$
- Group 7: $A_{18}, A_{19}, A_{20}, A_{21}$
- Group 8: $A_{22}, A_{23}, A_{24}, A_{25}$

The other variables which affects on this problem are as follows:

- $p = 0.0272$ N/cm$^3$ (0.1 lb/in.$^3$)
- $E$ = 68 947 MPa (10 000 Ksi)

**Table 17**
Comparison of best solution obtained from different algorithms for welded beam design problem.

| Algorithms | Optimum variables | | | | Optimum cost |
|---|---|---|---|---|---|
| | $h$ | $l$ | $t$ | $b$ | |
| TSA | 0.203290 | 3.471140 | 9.035100 | 0.201150 | **1.721020** |
| EPO | 0.205411 | 3.472341 | 9.035215 | 0.201153 | 1.723589 |
| SHO | 0.205563 | 3.474846 | 9.035799 | 0.205811 | 1.725661 |
| GWO | 0.205678 | 3.475403 | 9.036964 | 0.206229 | 1.726995 |
| PSO | 0.197411 | 3.315061 | 10.00000 | 0.201395 | 1.820395 |
| MVO | 0.205611 | 3.472103 | 9.040931 | 0.205709 | 1.725472 |
| SCA | 0.204695 | 3.536291 | 9.004290 | 0.210025 | 1.759173 |
| GSA | 0.147098 | 5.490744 | 10.00000 | 0.217725 | 2.172858 |
| GA | 0.164171 | 4.032541 | 10.00000 | 0.223647 | 1.873971 |

**Table 18**
Statistical results obtained from different algorithms for welded beam design problem.

| Algorithms | Best | Mean | Worst | Std. Dev. | Median |
|---|---|---|---|---|---|
| TSA | **1.721020** | **1.725021** | 1.727205 | 0.003316 | **1.724224** |
| EPO | 1.723589 | 1.725124 | 1.727211 | 0.004325 | 1.724399 |
| SHO | 1.725661 | 1.725828 | 1.726064 | **0.000287** | 1.725787 |
| GWO | 1.726995 | 1.727128 | 1.727564 | 0.001157 | 1.727087 |
| PSO | 1.820395 | 2.230310 | **3.048231** | 0.324525 | 2.244663 |
| MVO | 1.725472 | 1.729680 | 1.741651 | 0.004866 | 1.727420 |
| SCA | 1.759173 | 1.817657 | 1.873408 | 0.027543 | 1.820128 |
| GSA | 2.172858 | 2.544239 | 3.003657 | 0.255859 | 2.495114 |
| GA | 1.873971 | 2.119240 | 2.320125 | 0.034820 | 2.097048 |

**Table 19**
Comparison of best solution obtained from different algorithms for tension/compression spring design problem.

| Algorithms | Optimum variables | | | Optimum cost |
|---|---|---|---|---|
| | $d$ | $D$ | $P$ | |
| TSA | 0.051080 | 0.342890 | 12.0890 | **0.012655520** |
| EPO | 0.051087 | 0.342908 | 12.0898 | 0.012656987 |
| SHO | 0.051144 | 0.343751 | 12.0955 | 0.012674000 |
| GWO | 0.050178 | 0.341541 | 12.07349 | 0.012678321 |
| PSO | 0.05000 | 0.310414 | 15.0000 | 0.013192580 |
| MVO | 0.05000 | 0.315956 | 14.22623 | 0.012816930 |
| SCA | 0.050780 | 0.334779 | 12.72269 | 0.012709667 |
| GSA | 0.05000 | 0.317312 | 14.22867 | 0.012873881 |
| GA | 0.05010 | 0.310111 | 14.0000 | 0.013036251 |

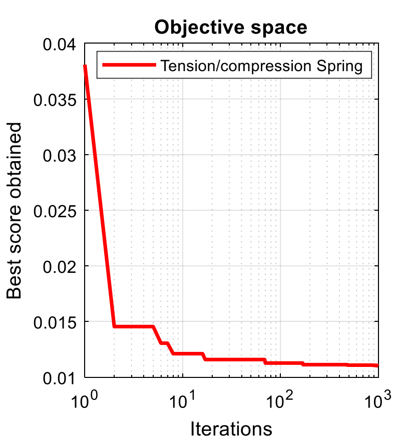


**Fig. 18.** Convergence analysis of TSA for tension/compression spring design problem.

- Displacement limitation = 0.35 in.
- Maximum displacement = 0.3504 in.
- Design variable set = $\{0.1, 0.2, 0.3, 0.4, 0.5, 0.6, 0.7, 0.8, 0.9, 1.0, 1.1, 1.2, 1.3, 1.4, 1.5, 1.6, 1.7, 1.8, 1.9, 2.0, 2.1, 2.2, 2.3, 2.4, 2.6, 2.8, 3.0, 3.2, 3.4\}$

Table 21 shows the member stress limitations for this problem.

*5.1.6. Rolling element bearing design problem*

The objective of this design problem is to maximize the dynamic load carrying capacity of a rolling element bearing as shown in Fig. 21. There are 10 decision variables such as pitch diameter ($D_m$), ball diameter ($D_b$), number of balls ($Z$), inner ($f_i$) and outer ($f_o$) raceway curvature coefficients, $K_{Dmin}$, $K_{Dmax}$, $\varepsilon$, $e$, and $\zeta$ (see Fig. 21). The mathematical justification of this problem is described below:

$$\text{Maximize } C_d = \begin{cases} f_c Z^{2/3} D_b^{1.8}, & if\ \ D \leq 25.4 \text{ mm} \\ C_d = 3.647 f_c Z^{2/3} D_b^{1.4}, & if\ \ D > 25.4 \text{ mm} \end{cases}$$

Subject to:

$$\begin{aligned}
g_1(\vec{z}) &= \frac{\phi_0}{2sin^{-1}(D_b/D_m)} - Z + 1 \leq 0,\\
g_2(\vec{z}) &= 2D_b - K_{Dmin}(D-d) \geq 0,\\
g_3(\vec{z}) &= K_{Dmax}(D-d) - 2D_b \geq 0,\\
g_4(\vec{z}) &= \zeta B_w - D_b \leq 0,\\
g_5(\vec{z}) &= D_m - 0.5(D+d) \geq 0,\\
g_6(\vec{z}) &= (0.5+e)(D+d) - D_m \geq 0,\\
g_7(\vec{z}) &= 0.5(D - D_m - D_b) - \varepsilon D_b \geq 0,\\
g_8(\vec{z}) &= f_i \geq 0.515,\\
g_9(\vec{z}) &= f_o \geq 0.515,
\end{aligned} \tag{12}$$

where,

$$f_c = 37.91\left[1 + \left\{1.04\left(\frac{1-\gamma}{1+\gamma}\right)^{1.72}\left(\frac{f_i(2f_o-1)}{f_o(2f_i-1)}\right)^{0.41}\right\}^{10/3}\right]^{-0.3}$$

$$\times\left[\frac{\gamma^{0.3}(1-\gamma)^{1.39}}{(1+\gamma)^{1/3}}\right]\left[\frac{2f_i}{2f_i-1}\right]^{0.41}$$

$$x = [\{(D-d)/2 - 3(T/4)\}^2 + \{D/2 - T/4 - D_b\}^2 - \{d/2 + T/4\}^2]$$

$$y = 2\{(D-d)/2 - 3(T/4)\}\{D/2 - T/4 - D_b\}$$

$$\phi_o = 2\pi - 2cos^{-1}\left(\frac{x}{y}\right)$$

$$\gamma = \frac{D_b}{D_m}, \quad f_i = \frac{r_i}{D_b}, \quad f_o = \frac{r_o}{D_b}, \quad T = D - d - 2D_b$$

$$D = 160, \quad d = 90, \quad B_w = 30, \quad r_i = r_o = 11.033$$

$$0.5(D+d) \leq D_m \leq 0.6(D+d), \quad 0.15(D-d) \leq D_b$$

$$\leq 0.45(D-d), \quad 4 \leq Z \leq 50, \quad 0.515 \leq f_i \ and\ f_o \leq 0.6,$$

$$0.4 \leq K_{Dmin} \leq 0.5, \quad 0.6 \leq K_{Dmax} \leq 0.7, \quad 0.3 \leq e \leq 0.4,$$

$$0.02 \leq e \leq 0.1, \quad 0.6 \leq \zeta \leq 0.85.$$

Table 24 presents the performance of best obtained optimal solution between proposed and other algorithms. TSA obtains the optimal solution at $z_{1-10} = (125, 21.41750, 10.94109, 0.510, 0.515, 0.4, 0.7, 0.3, 0.02, 0.6)$ with corresponding fitness value as $f(z_{1-10}) = 85\,070.085$. The statistical results for rolling element bearing design problem are tabulated in Table 25. The results reveal that TSA generates the best optimal solution with continuous improvements.

Table 22 shows the loading conditions for 25-bar truss problem. The comparison of best obtained solutions is tabulated in Table 23. It is

**Table 20**
Statistical results obtained from different algorithms for tension/compression spring design problem.

| Algorithms | Best | Mean | Worst | Std. Dev. | Median |
|---|---|---|---|---|---|
| TSA | **0.012655520** | **0.012677560** | 0.012667890 | 0.001010 | **0.012675990** |
| EPO | 0.012656987 | 0.012678903 | 0.012667902 | 0.001021 | 0.012676002 |
| SHO | 0.012674000 | 0.012684106 | 0.012715185 | **0.000027** | 0.012687293 |
| GWO | 0.012678321 | 0.012697116 | 0.012720757 | 0.000041 | 0.012699686 |
| PSO | 0.013192580 | 0.014817181 | **0.017862507** | 0.002272 | 0.013192580 |
| MVO | 0.012816930 | 0.014464372 | 0.017839737 | 0.001622 | 0.014021237 |
| SCA | 0.012709667 | 0.012839637 | 0.012998448 | 0.000078 | 0.012844664 |
| GSA | 0.012873881 | 0.013438871 | 0.014211731 | 0.000287 | 0.013367888 |
| GA | 0.013036251 | 0.014036254 | 0.016251423 | 0.002073 | 0.013002365 |

**Table 21**
Member stress limitations for 25-bar truss design problem.

| Element group | Compressive stress limitations Ksi (MPa) | Tensile stress limitations Ksi (MPa) |
|---|---|---|
| Group 1 | 35.092 (241.96) | 40.0 (275.80) |
| Group 2 | 11.590 (79.913) | 40.0 (275.80) |
| Group 3 | 17.305 (119.31) | 40.0 (275.80) |
| Group 4 | 35.092 (241.96) | 40.0 (275.80) |
| Group 5 | 35.092 (241.96) | 40.0 (275.80) |
| Group 6 | 6.759 (46.603) | 40.0 (275.80) |
| Group 7 | 6.959 (47.982) | 40.0 (275.80) |
| Group 8 | 11.082 (76.410) | 40.0 (275.80) |

analyzed that the proposed TSA is better than other algorithms in terms of best, average, and standard deviation. TSA converges very efficiently towards optimal design of this problem as shown in Fig. 20.

Fig. 22 reveals the convergence behavior of TSA algorithm and it can be seen that TSA is able to achieve best optimal design.

### 5.2. Unconstrained engineering problem

This subsection describes the displacement of loaded structure design problem to minimize the potential energy.

#### 5.2.1. Displacement of loaded structure design problem

A displacement is a vector which defines the shortest distance between the initial and final position of a given point. The main objective of this unconstrained problem is to minimize the potential energy for reducing the excess load of structure. The loaded structure that should have minimum potential energy ($f(\vec{z})$) is depicted in Fig. 23. The problem can be justified as follows:

$$f(\vec{z}) = \text{Minimize}_{z_1,z_2}\ \pi$$

where,

$$\pi = \frac{1}{2}K_1u_1^2 + \frac{1}{2}K_2u_2^2 - F_zz_1 - F_yz_2 \tag{13}$$

$$K_1 = 8\ \text{N/cm},\ K_2 = 1\ \text{N/cm},\ F_y = 5\ \text{N},\ F_z = 5\ \text{N}$$

$$u_1 = \sqrt{z_1^2 + (10 - z_2^2)} - 10, \quad u_2 = \sqrt{z_1^2 + (10 + z_2^2)} - 10.$$

Table 26 shows the best comparison of optimal solutions obtained from the proposed TSA and other algorithms. TSA achieves best optimum cost at $\pi = 167.2635$. It can be analyzed that TSA is able to minimize the potential energy for loaded structure problem. The statistical results are also given in Table 27. It can be seen that TSA are better than the other metaheuristics in terms of best, mean, and median. Fig. 24 shows the convergence behavior of best optimal design obtained from TSA algorithm.

Overall, TSA is an efficient and effective optimizer for solving both constrained and unconstrained engineering design problems.

## 6. Conclusion and future scope

In this paper, we presented a bio-inspired based bio-inspired metaheuristic algorithm called Tunicate Swarm Algorithm (TSA). The fundamental inspiration of this algorithm includes the jet propulsion and swarm behaviors of tunicate. The proposed algorithm is experimented on a set of seventy-four benchmark test functions belonging to classical, CEC-2015 and CEC-2017 test suite. The statistical results proved the

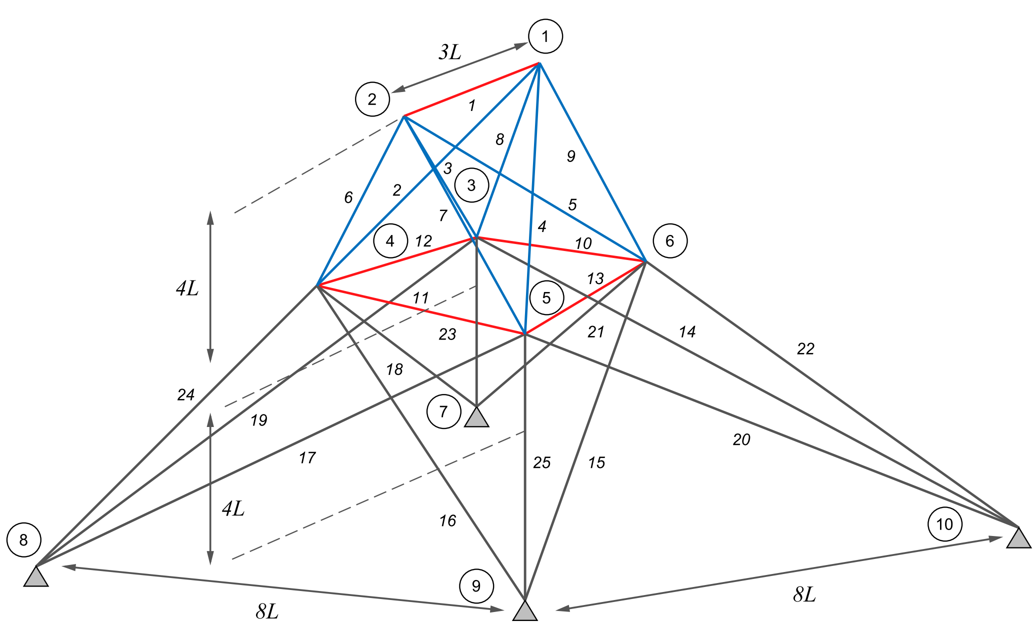


**Fig. 19.** Schematic view of 25-bar truss problem.

**Table 22**
Two loading conditions for the 25-bar truss design problem.

| Node | Case 1 | | | Case 2 | | |
|---|---|---|---|---|---|---|
| | $P_x Kips(kN)$ | $P_y Kips(kN)$ | $P_z Kips(kN)$ | $P_x Kips(kN)$ | $P_y Kips(kN)$ | $P_z Kips(kN)$ |
| 1 | 0.0 | 20.0 (89) | −5.0 (22.25) | 1.0 (4.45) | 10.0 (44.5) | −5.0 (22.25) |
| 2 | 0.0 | −20.0 (89) | −5.0 (22.25) | 0.0 | 10.0 (44.5) | −5.0 (22.25) |
| 3 | 0.0 | 0.0 | 0.0 | 0.5 (2.22) | 0.0 | 0.0 |
| 6 | 0.0 | 0.0 | 0.0 | 0.5 (2.22) | 0.0 | 0.0 |

**Table 23**
Statistical results obtained from different algorithms for 25-bar truss design problem.

| Groups | TSA | ACO (Bichon, 2004) | PSO (Schutte and Groenwold, 2003) | CSS (Kaveh and Talatahari, 2010) | BB-BC (Kaveh and Talatahari, 2009c) |
|---|---|---|---|---|---|
| $A1$ | **0.01** | 0.01 | 0.01 | 0.01 | 0.01 |
| $A2-A5$ | **1.840** | 2.042 | 2.052 | 2.003 | 1.993 |
| $A6-A9$ | **3.001** | 3.001 | 3.001 | 3.007 | 3.056 |
| $A10-A11$ | **0.01** | 0.01 | 0.01 | 0.01 | 0.01 |
| $A12-A13$ | **0.01** | 0.01 | 0.01 | 0.01 | 0.01 |
| $A14-A17$ | **0.651** | 0.684 | 0.684 | 0.687 | 0.665 |
| $A18-A21$ | 1.620 | 1.625 | **1.616** | 1.655 | 1.642 |
| $A22-A25$ | 2.67 | 2.672 | 2.673 | **2.66** | 2.679 |
| **Best weight** | **544.80** | 545.03 | 545.21 | 545.10 | 545.16 |
| **Average weight** | **545.10** | 545.74 | 546.84 | 545.58 | 545.66 |
| **Std. dev.** | **0.391** | 0.94 | 1.478 | 0.412 | 0.491 |

**Table 24**
Comparison of best solution obtained from different algorithms for rolling element bearing design problem.

| Algorithms | Optimum variables | | | | | | | | | | Opt. cost |
|---|---|---|---|---|---|---|---|---|---|---|---|
| | $D_m$ | $D_b$ | $Z$ | $f_i$ | $f_o$ | $K_{Dmin}$ | $K_{Dmax}$ | $\varepsilon$ | $e$ | $\zeta$ | |
| TSA | 125 | 21.41750 | 10.94100 | 0.510 | 0.515 | 0.4 | 0.7 | 0.3 | 0.02 | 0.6 | **85070.080** |
| EPO | 125 | 21.41890 | 10.94113 | 0.515 | 0.515 | 0.4 | 0.7 | 0.3 | 0.02 | 0.6 | 85 067.983 |
| SHO | 125 | 21.40732 | 10.93268 | 0.515 | 0.515 | 0.4 | 0.7 | 0.3 | 0.02 | 0.6 | 85 054.532 |
| GWO | 125.6199 | 21.35129 | 10.98781 | 0.515 | 0.515 | 0.5 | 0.68807 | 0.300151 | 0.03254 | 0.62701 | 84 807.111 |
| PSO | 125 | 20.75388 | 11.17342 | 0.515 | 0.515000 | 0.5 | 0.61503 | 0.300000 | 0.05161 | 0.60000 | 81 691.202 |
| MVO | 125.6002 | 21.32250 | 10.97338 | 0.515 | 0.515000 | 0.5 | 0.68782 | 0.301348 | 0.03617 | 0.61061 | 84 491.266 |
| SCA | 125 | 21.14834 | 10.96928 | 0.515 | 0.515 | 0.5 | 0.7 | 0.3 | 0.02778 | 0.62912 | 83 431.117 |
| GSA | 125 | 20.85417 | 11.14989 | 0.515 | 0.517746 | 0.5 | 0.61827 | 0.304068 | 0.02000 | 0.624638 | 82 276.941 |
| GA | 125 | 20.77562 | 11.01247 | 0.515 | 0.515000 | 0.5 | 0.61397 | 0.300000 | 0.05004 | 0.610001 | 82 773.982 |

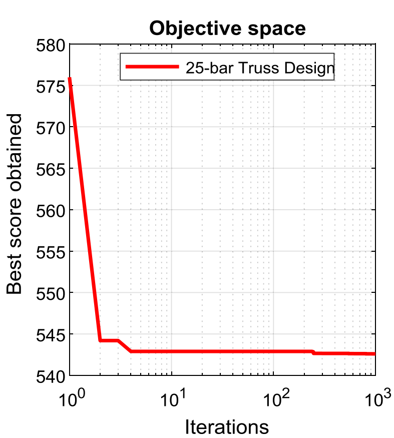


**Fig. 20.** Convergence analysis of TSA for 25-bar truss design problem.

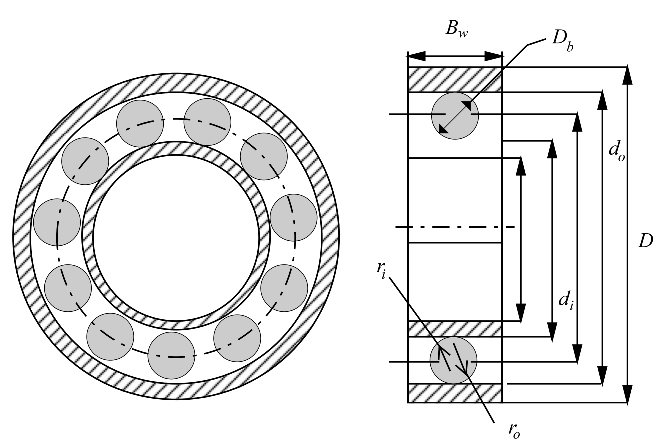


**Fig. 21.** Schematic view of rolling element bearing problem.

effectiveness of TSA towards attaining global optimal solutions having better convergence in comparison to its rivals.

For CEC-2015 and CEC-2017 benchmark test functions, all the competitor algorithms rarely found the global optimal solutions, contrarily the performance of TSA is found to be accurate and consistent. We also investigated the effect of scalability and sensitivity on efficacy of TSA and the simulation results reveal that the proposed algorithm is less susceptible as compared to other algorithms. In addition, the effectiveness and efficiency of TSA is also demonstrated by applying it on six constrained and one unconstrained engineering design problems. From the experimental outcomes, it can be concluded that the proposed TSA is applicable to real-world case studies with unknown search spaces.

This paper opens several research directions like TSA may be extended in future to solve multi-objective optimization problems. Apart

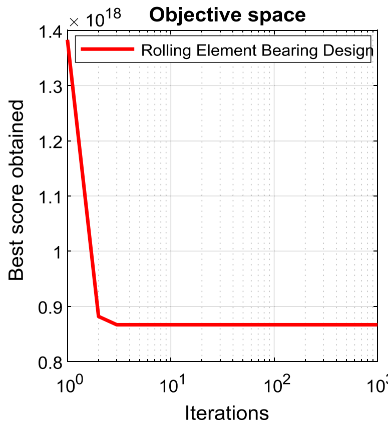


**Fig. 22.** Convergence analysis of TSA for rolling element bearing design problem.

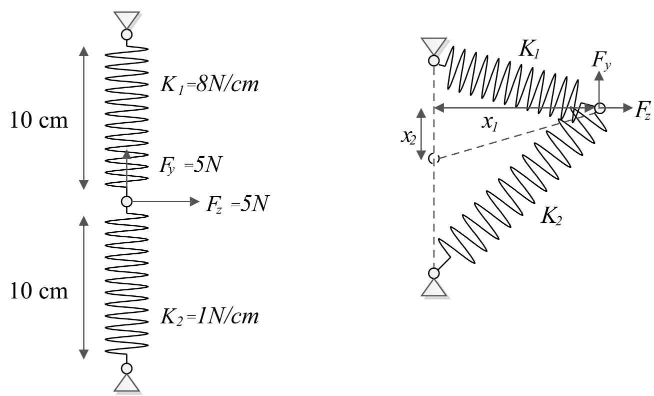


**Fig. 23.** Schematic view of displacement of loaded structure.

**Table 25**
Statistical results obtained from different algorithms for rolling element bearing design problem.

| Algorithms | Best | Mean | Worst | Std. Dev. | Median |
|---|---|---|---|---|---|
| TSA | **85 070.080** | **85 044.951** | 86 552.480 | 1976.21 | **85 058.162** |
| EPO | 85 067.983 | 85 042.352 | 86 551.599 | 1877.09 | 85 056.095 |
| SHO | 85 054.532 | 85 024.858 | 85 853.876 | 0186.68 | 85 040.241 |
| GWO | 84 807.111 | 84 791.613 | 84 517.923 | 0137.186 | 84 960.147 |
| PSO | 81 691.202 | 50 435.017 | **32761.546** | **13 962.150** | 42 287.581 |
| MVO | 84 491.266 | 84 353.685 | 84 100.834 | 0392.431 | 84 398.601 |
| SCA | 83 431.117 | 81 005.232 | 77 992.482 | 1710.777 | 81 035.109 |
| GSA | 82 276.941 | 78 002.107 | 71 043.110 | 3119.904 | 78 398.853 |
| GA | 82 773.982 | 81 198.753 | 80 687.239 | 1679.367 | 8439.728 |

**Table 26**
Comparison of best solution obtained from different algorithms for displacement of loaded structure problem.

| Algorithms | Optimum cost ($\pi$) |
|---|---|
| TSA | **167.0024** |
| EPO | 168.8231 |
| SHO | 168.8889 |
| GWO | 170.3645 |
| PSO | 170.5960 |
| MVO | 169.3023 |
| SCA | 169.0032 |
| GSA | 176.3697 |
| GA | 171.3674 |

from this, the proposal of binary or many objective versions of TSA could be some significant contributions as well.

**Table 27**
Statistical results obtained from different algorithms for displacement of loaded structure problem.

| Algorithms | Best | Mean | Worst | Std. Dev. | Median |
|---|---|---|---|---|---|
| TSA | **167.0024** | **169.5302** | 176.1111 | 208.823 | **168.5217** |
| EPO | 168.8231 | 170.1309 | **230.9721** | 211.861 | 169.4214 |
| SHO | 168.8889 | 170.3659 | 173.6357 | **023.697** | 169.6710 |
| GWO | 170.3645 | 171.3694 | 174.3970 | 196.037 | 173.3694 |
| PSO | 170.5960 | 174.6354 | 175.3602 | 236.036 | 173.9634 |
| MVO | 169.3023 | 171.0034 | 174.3047 | 202.753 | 170.0032 |
| SCA | 169.0032 | 171.7530 | 174.4527 | 129.047 | 170.3647 |
| GSA | 176.3697 | 178.7521 | 179.5637 | 113.037 | 174.367 |
| GA | 171.3674 | 172.0374 | 174.0098 | 212.703 | 172.0097 |

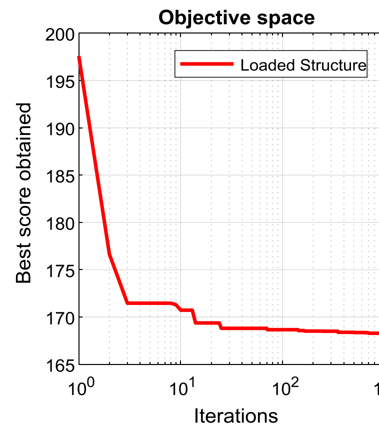


**Fig. 24.** Convergence analysis of TSA for displacement of loaded structure problem.

## CRediT authorship contribution statement

Satnam Kaur conceptualize the data and write the paper, Lalit K. Awasthi proposed the methodology, A.L. Sangal simulate the software, and Gaurav Dhiman investigate the proposed algorithm.

## Acknowledgment

The corresponding author, **Dr. Gaurav Dhiman**, would like to thanks to the goddess **SHRI MATA VAISHNO DEVI** for her divine blessings on him.

## Appendix. Unimodal, multimodal, and fixed-dimension multimodal benchmark test functions

### *A.1. Unimodal benchmark test functions*

#### *A.1.1. Sphere model*

$$F_1(z) = \sum_{i=1}^{30} z_i^2$$

$$-100 \leq z_i \leq 100, \quad f_{min} = 0, \quad Dim = 30$$

#### *A.1.2. Schwefel's problem 2.22*

$$F_2(z) = \sum_{i=1}^{30} |z_i| + \prod_{i=1}^{30} |z_i|$$

$$-10 \leq z_i \leq 10, \quad f_{min} = 0, \quad Dim = 30$$

**Table 28**
Shekel's Foxholes function $F_{14}$.

| $(a_{ij}, i = 1, 2$ and $j = 1, 2, \ldots, 25)$ | | | | | | | | |
|---|---|---|---|---|---|---|---|---|
| $i \backslash j$ | 1 | 2 | 3 | 4 | 5 | 6 | … | 25 |
| 1 | −32 | −16 | 0 | 16 | 32 | −32 | … | 32 |
| 2 | −32 | −32 | −32 | −32 | −32 | −16 | … | 32 |

**Table 29**
Hartman function $F_{19}$.

| $i$ | $(a_{ij}, j = 1, 2, 3)$ | | | $c_i$ | $(p_{ij}, j = 1, 2, 3)$ | | |
|---|---|---|---|---|---|---|---|
| 1 | 3 | 10 | 30 | 1 | 0.3689 | 0.1170 | 0.2673 |
| 2 | 0.1 | 10 | 35 | 1.2 | 0.4699 | 0.4387 | 0.7470 |
| 3 | 3 | 10 | 30 | 3 | 0.1091 | 0.8732 | 0.5547 |
| 4 | 0.1 | 10 | 35 | 3.2 | 0.038150 | 0.5743 | 0.8828 |

**Table 30**
Shekel Foxholes functions $F_{21}, F_{22}, F_{23}$.

| $i$ | $(a_{ij}, j = 1, 2, 3, 4)$ | | | | $c_i$ |
|---|---|---|---|---|---|
| 1 | 4 | 4 | 4 | 4 | 0.1 |
| 2 | 1 | 1 | 1 | 1 | 0.2 |
| 3 | 8 | 8 | 8 | 8 | 0.2 |
| 4 | 6 | 6 | 6 | 6 | 0.4 |
| 5 | 3 | 7 | 3 | 7 | 0.4 |
| 6 | 2 | 9 | 2 | 9 | 0.6 |
| 7 | 5 | 5 | 3 | 3 | 0.3 |
| 8 | 8 | 1 | 8 | 1 | 0.7 |
| 9 | 6 | 2 | 6 | 2 | 0.5 |
| 10 | 7 | 3.6 | 7 | 3.6 | 0.5 |

### *A.1.3. Schwefel's problem 1.2*

$$F_3(z) = \sum_{i=1}^{30}\left(\sum_{j=1}^{i} z_j\right)^2$$

$-100 \le z_i \le 100, \quad f_{min} = 0, \quad Dim = 30$

### *A.1.4. Schwefel's problem 2.21*

$$F_4(z) = max_i\{|z_i|, 1 \le i \le 30\}$$

$-100 \le z_i \le 100, \quad f_{min} = 0, \quad Dim = 30$

### *A.1.5. Generalized Rosenbrock's function*

$$F_5(z) = \sum_{i=1}^{29}[100(z_{i+1} - z_i^2)^2 + (z_i - 1)^2]$$

$-30 \le z_i \le 30, \quad f_{min} = 0, \quad Dim = 30$

### *A.1.6. Step function*

$$F_6(z) = \sum_{i=1}^{30}(\lfloor z_i + 0.5 \rfloor)^2$$

$-100 \le z_i \le 100, \quad f_{min} = 0, \quad Dim = 30$

### *A.1.7. Quartic function*

$$F_7(z) = \sum_{i=1}^{30} i z_i^4 + random[0, 1]$$

$-1.28 \le z_i \le 1.28, \quad f_{min} = 0, \quad Dim = 30$

## *A.2. Multimodal benchmark test functions*

### *A.2.1. Generalized Schwefel's problem 2.26*

$$F_8(z) = \sum_{i=1}^{30} -z_i sin(\sqrt{|z_i|})$$

$-500 \le z_i \le 500, \quad f_{min} = -12\,569.5, \quad Dim = 30$

### *A.2.2. Generalized Rastrigin's function*

$$F_9(z) = \sum_{i=1}^{30}[z_i^2 - 10cos(2\pi z_i) + 10]$$

$-5.12 \le z_i \le 5.12, \quad f_{min} = 0, \quad Dim = 30$

### *A.2.3. Ackley's function*

$$F_{10}(z) = -20exp\left(-0.2\sqrt{\frac{1}{30}\sum_{i=1}^{30} z_i^2}\right) - exp\left(\frac{1}{30}\sum_{i=1}^{30} cos(2\pi z_i)\right) + 20 + e$$
$$-32 \le z_i \le 32, \quad f_{min} = 0, \quad Dim = 30$$

### *A.2.4. Generalized Griewank function*

$$F_{11}(z) = \frac{1}{4000}\sum_{i=1}^{30} z_i^2 - \prod_{i=1}^{30} cos\left(\frac{z_i}{\sqrt{i}}\right) + 1$$

$-600 \le z_i \le 600, \quad f_{min} = 0, \quad Dim = 30$

### *A.2.5. Generalized Penalized functions*

- $$F_{12}(z) = \frac{\pi}{30}\{10sin(\pi x_1) + \sum_{i=1}^{29}(x_i - 1)^2[1 + 10sin^2(\pi x_{i+1})] + (x_n - 1)^2\} + \sum_{i=1}^{30} u(z_i, 10, 100, 4)$$
  $$-50 \le z_i \le 50, \quad f_{min} = 0, \quad Dim = 30$$

- $$F_{13}(z) = 0.1\{sin^2(3\pi z_1) + \sum_{i=1}^{29}(z_i - 1)^2[1 + sin^2(3\pi z_i + 1)] + (z_n - 1)^2 \times [1 + sin^2(2\pi z_{30})]\} + \sum_{i=1}^{N} u(z_i, 5, 100, 4)$$
  $$-50 \le z_i \le 50, \quad f_{min} = 0, \quad Dim = 30$$

  where, $x_i = 1 + \frac{z_i + 1}{4}$

  $$u(z_i, a, k, m) = \begin{cases} k(z_i - a)^m & z_i > a \\ 0 & -a < z_i < a \\ k(-z_i - a)^m & z_i < -a \end{cases}$$

## *A.3. Fixed-dimension multimodal benchmark test functions*

### *A.3.1. Shekel's Foxholes function*

See Table 28.

$$F_{14}(z) = \left(\frac{1}{500} + \sum_{j=1}^{25}\frac{1}{j + \sum_{i=1}^{2}(z_i - a_{ij})^6}\right)^{-1}$$

$-65.536 \le z_i \le 65.536, \quad f_{min} \approx 1, \quad Dim = 2$

**Table 31**
Hartman function $F_{20}$.

| $i$ | ($a_{ij}, j = 1, 2, \ldots, 6$) | | | | | | $c_i$ | ($p_{ij}, j = 1, 2, \ldots, 6$) | | | | | |
|---|---|---|---|---|---|---|---|---|---|---|---|---|---|
| 1 | 10 | 3 | 17 | 3.5 | 1.7 | 8 | 1 | 0.1312 | 0.1696 | 0.5569 | 0.0124 | 0.8283 | 0.5886 |
| 2 | 0.05 | 10 | 17 | 0.1 | 8 | 14 | 1.2 | 0.2329 | 0.4135 | 0.8307 | 0.3736 | 0.1004 | 0.9991 |
| 3 | 3 | 3.5 | 1.7 | 10 | 17 | 8 | 3 | 0.2348 | 0.1415 | 0.3522 | 0.2883 | 0.3047 | 0.6650 |
| 4 | 17 | 8 | 0.05 | 10 | 0.1 | 14 | 3.2 | 0.4047 | 0.8828 | 0.8732 | 0.5743 | 0.1091 | 0.0381 |

**Table A.1**
Composite benchmark test functions.

| Functions | Dim | Range | $f_{min}$ |
|---|---|---|---|
| $F_{24}(CF1)$ :<br>$f_1, f_2, f_3, \ldots, f_{10}$ = Sphere function<br>$[\alpha_1, \alpha_2, \alpha_3, \ldots, \alpha_{10}] = [1, 1, 1, \ldots, 1]$<br>$[\beta_1, \beta_2, \beta_3, \ldots, \beta_{10}] = [5/100, 5/100, 5/100, \ldots, 5/100]$ | 10 | $[-5, 5]$ | 0 |
| $F_{25}(CF2)$ :<br>$f_1, f_2, f_3, \ldots, f_{10}$ = Griewank's Function<br>$[\alpha_1, \alpha_2, \alpha_3, \ldots, \alpha_{10}] = [1, 1, 1, \ldots, 1]$<br>$[\beta_1, \beta_2, \beta_3, \ldots, \beta_{10}] = [5/100, 5/100, 5/100, \ldots, 5/100]$ | 10 | $[-5, 5]$ | 0 |
| $F_{26}(CF3)$ :<br>$f_1, f_2$ = Ackley's Function<br>$f_1, f_2, f_3, \ldots, f_{10}$ = Griewank's Function<br>$[\alpha_1, \alpha_2, \alpha_3, \ldots, \alpha_{10}] = [1, 1, 1, \ldots, 1]$<br>$[\beta_1, \beta_2, \beta_3, \ldots, \beta_{10}] = [1, 1, 1, \ldots, 1]$ | 10 | $[-5, 5]$ | 0 |
| $F_{27}(CF4)$ :<br>$f_1, f_2$ = Ackley's Function<br>$f_3, f_4$ = Rastrigin's Function<br>$f_5, f_6$ = Weierstras's Function<br>$f_7, f_8$ = Griewank's Function<br>$f_9, f_{10}$ = Sphere Function<br>$[\alpha_1, \alpha_2, \alpha_3, \ldots, \alpha_{10}] = [1, 1, 1, \ldots, 1]$<br>$[\beta_1, \beta_2, \beta_3, \ldots, \beta_{10}] = [5/32, 5/32, 1, 1, 5/0.5, 5/0.5, 5/100, 5/100, 5/100, 5/100]$ | 10 | $[-5, 5]$ | 0 |
| $F_{28}(CF5)$ :<br>$f_1, f_2$ = Rastrigin's Function<br>$f_3, f_4$ = Weierstras's Function<br>$f_5, f_6$ = Griewank's Function<br>$f_7, f_8$ = Ackley's Function<br>$f_9, f_{10}$ = Sphere Function<br>$[\alpha_1, \alpha_2, \alpha_3, \ldots, \alpha_{10}] = [1, 1, 1, \ldots, 1]$<br>$[\beta_1, \beta_2, \beta_3, \ldots, \beta_{10}] = [1/5, 1/5, 5/0.5, 5/0.5, 5/100, 5/100, 5/32, 5/32, 5/100, 5/100]$ | 10 | $[-5, 5]$ | 0 |
| $F_{29}(CF6)$ :<br>$f_1, f_2$ = Rastrigin's Function<br>$f_3, f_4$ = Weierstras's Function<br>$f_5, f_6$ = Griewank's Function<br>$f_7, f_8$ = Ackley's Function<br>$f_9, f_{10}$ = Sphere Function<br>$[\alpha_1, \alpha_2, \alpha_3, \ldots, \alpha_{10}] = [0.1, 0.2, 0.3, 0.4, 0.5, 0.6, 0.7, 0.8, 0.9, 1]$<br>$[\beta_1, \beta_2, \beta_3, \ldots, \beta_{10}] =$<br>$[0.1 * 1/5, 0.2 * 1/5, 0.3 * 5/0.5, 0.4 * 5/0.5, 0.5 * 5/100, 0.6 * 5/100, 0.7 * 5/32, 0.8 * 5/32, 0.9 * 5/100, 1 * 5/100]$ | 10 | $[-5, 5]$ | 0 |

#### A.3.2. Kowalik's function

$$F_{15}(z) = \sum_{i=1}^{11}\left[a_i - \frac{z_1(b_i^2 + b_i z_2)}{b_i^2 + b_i z_3 + z_4}\right]^2$$

$$-5 \leq z_i \leq 5, \quad f_{min} \approx 0.0003075, \quad Dim = 4$$

#### A.3.3. Six-Hump Camel-Back function

$$F_{16}(z) = 4z_1^2 - 2.1z_1^4 + \frac{1}{3}z_1^6 + z_1 z_2 - 4z_2^2 + 4z_2^4$$

$$-5 \leq z_i \leq 5, \quad f_{min} = -1.0316285, \quad Dim = 2$$

#### A.3.4. Branin function

$$F_{17}(z) = \left(z_2 - \frac{5.1}{4\pi^2}z_1^2 + \frac{5}{\pi}z_1 - 6\right)^2 + 10\left(1 - \frac{1}{8\pi}\right)cos z_1 + 10$$

$$-5 \leq z_1 \leq 10, \quad 0 \leq z_2 \leq 15, \quad f_{min} = 0.398, \quad Dim = 2$$

#### A.3.5. Goldstein–price function

$$\begin{aligned} F_{18}(z) = {} & [1 + (z_1 + z_2 + 1)^2(19 - 14z_1 + 3z_1^2 - 14z_2 + 6z_1 z_2 + 3z_2^2)] \\ & \times [30 + (2z_1 - 3z_2)^2 \times (18 - 32z_1 + 12z_1^2 + 48z_2 \\ & - 36z_1 z_2 + 27z_2^2)] \\ & -2 \leq z_i \leq 2, \quad f_{min} = 3, \quad Dim = 2 \end{aligned}$$

#### A.3.6. Hartman's family

- $F_{19}(z) = -\sum_{i=1}^{4} c_i exp(-\sum_{j=1}^{3} a_{ij}(z_j - p_{ij})^2)$ $0 \leq z_j \leq 1$, $f_{min} = -3.86$, $Dim = 3$
- $F_{20}(z) = -\sum_{i=1}^{4} c_i exp(-\sum_{j=1}^{6} a_{ij}(z_j - p_{ij})^2)$ $0 \leq z_j \leq 1$, $f_{min} = -3.32$, $Dim = 6$ (see Table 29).

#### A.3.7. Shekel's Foxholes function

- $F_{21}(z) = -\sum_{i=1}^{5}[(X - a_i)(X - a_i)^T + c_i]^{-1}$ $0 \leq z_i \leq 10$, $f_{min} = -10.1532$, $Dim = 4$
- $F_{22}(z) = -\sum_{i=1}^{7}[(X - a_i)(X - a_i)^T + c_i]^{-1}$ $0 \leq z_i \leq 10$, $f_{min} = -10.4028$, $Dim = 4$
- $F_{23}(z) = -\sum_{i=1}^{10}[(X - a_i)(X - a_i)^T + c_i]^{-1}$ $0 \leq z_i \leq 10$, $f_{min} = -10.536$, $Dim = 4$ (see Tables 30 and 31).

**Table A.2**
IEEE CEC-2015 benchmark test functions.

| No. | Functions | Related basic functions | Dim | $f_{min}$ |
|---|---|---|---|---|
| $CEC-1$ | Rotated Bent Cigar Function | Bent Cigar Function | 30 | 100 |
| $CEC-2$ | Rotated Discus Function | Discus Function | 30 | 200 |
| $CEC-3$ | Shifted and Rotated Weierstrass Function | Weierstrass Function | 30 | 300 |
| $CEC-4$ | Shifted and Rotated Schwefel's Function | Schwefel's Function | 30 | 400 |
| $CEC-5$ | Shifted and Rotated Katsuura Function | Katsuura Function | 30 | 500 |
| $CEC-6$ | Shifted and Rotated HappyCat Function | HappyCat Function | 30 | 600 |
| $CEC-7$ | Shifted and Rotated HGBat Function | HGBat Function | 30 | 700 |
| $CEC-8$ | Shifted and Rotated Expanded Griewank's plus Rosenbrock's Function | Griewank's Function<br>Rosenbrock's Function | 30 | 800 |
| $CEC-9$ | Shifted and Rotated Expanded Scaffer's F6 Function | Expanded Scaffer's F6 Function | 30 | 900 |
| $CEC-10$ | Hybrid Function 1 ($N=3$) | Schwefel's Function<br>Rastrigin's Function<br>High Conditioned Elliptic Function | 30 | 1000 |
| $CEC-11$ | Hybrid Function 2 ($N=4$) | Griewank's Function<br>Weierstrass Function<br>Rosenbrock's Function<br>Scaffer's F6 Function | 30 | 1100 |
| $CEC-12$ | Hybrid Function 3 ($N=5$) | Katsuura Function<br>HappyCat Function<br>Expanded Griewank's plus Rosenbrock's Function<br>Schwefel's Function<br>Ackley's Function | 30 | 1200 |
| $CEC-13$ | Composition Function 1 ($N=5$) | Rosenbrock's Function<br>High Conditioned Elliptic Function<br>Bent Cigar Function<br>Discus Function<br>High Conditioned Elliptic Function | 30 | 1300 |
| $CEC-14$ | Composition Function 2 ($N=3$) | Schwefel's Function<br>Rastrigin's Function<br>High Conditioned Elliptic Function | 30 | 1400 |
| $CEC-15$ | Composition Function 3 ($N=5$) | HGBat Function<br>Rastrigin's Function<br>Schwefel's Function<br>Weierstrass Function<br>High Conditioned Elliptic Function | 30 | 1500 |

*A.4. Basic composite benchmark test functions*

*A.4.1. Weierstrass function*

$$F(z)=\sum_{i=1}^{30}\Big(\sum_{k=0}^{20}[0.5^k cos(2\pi 3^k(z_i+0.5))]\Big)-30\sum_{k=0}^{20}[0.5^k cos(2\pi 3^k\times 0.5)]$$

Note that the Sphere, Rastrigin's, Griewank's, and Ackley's functions in composite benchmark suite are same as above mentioned $F_1, F_9, F_{11}$, and $F_{10}$ benchmark test functions.

*A.5. Basic CEC-2015 benchmark test functions*

*A.5.1. Bent Cigar function*

$$F(z)=z_1^2+10^6\sum_{i=2}^{30}z_i^2$$

*A.5.2. Discus function*

$$F(z)=10^6 z_1^2+\sum_{i=2}^{30}z_i^2$$

*A.5.3. Modified Schwefel's function*

$$F(z)=418.9829\times 30-\sum_{i=1}^{30}g(y_i),\quad y_i=z_i+4.209687462275036e+002$$

$$g(y_i)=\begin{cases} y_i sin(|y_i|^{1/2}) \\ \quad where, if\ |y_i|\le 500, \\ (500-mod(y_i,500))sin(\sqrt{|500-mod(y_i,500)|})-\dfrac{(y_i-500)^2}{10000\times 30} \\ \quad where, if\ y_i>500, \\ (mod(|y_i|,500)-500)sin(\sqrt{|mod(|y_i|,500)-500|})-\dfrac{(y_i+500)^2}{10000\times 30} \\ \quad where, if\ y_i<-500 \end{cases}$$

*A.5.4. Katsuura function*

$$F(z)=\frac{10}{30^2}\prod_{i=1}^{30}\Big(1+i\sum_{j=1}^{32}\frac{|2^j z_i-round(2^j z_i)|}{2^j}\Big)^{\frac{10}{30^{1.2}}}-\frac{10}{30^2}$$

*A.5.5. HappyCat function*

$$F(z)=\Big|\sum_{i=1}^{30}z_i^2-30\Big|^{1/4}+(0.5\sum_{i=1}^{30}z_i^2+\sum_{i=1}^{30}z_i)/30+0.5$$

*A.5.6. HGBat function*

$$F(z)=\Big|(\sum_{i=1}^{30}z_i^2)^2-(\sum_{i=1}^{30}z_i)^2\Big|^{1/2}+(0.5\sum_{i=1}^{30}z_i^2+\sum_{i=1}^{30}z_i)/30+0.5$$

*A.5.7. Expanded Griewank's plus Rosenbrock's function*

$$F(z)=F_{39}(F_{38}(z_1,z_2))+F_{39}(F_{38}(z_2,z_3))+\cdots+F_{39}(F_{38}(z_{30},z_1))$$

**Table A.3**
IEEE CEC-2017 benchmark test functions.

| No. | Functions | $f_{min}$ |
|---|---|---|
| $C-1$ | Shifted and Rotated Bent Cigar Function | 100 |
| $C-2$ | Shifted and Rotated Sum of Different Power Function | 200 |
| $C-3$ | Shifted and Rotated Zakharov Function | 300 |
| $C-4$ | Shifted and Rotated Rosenbrock's Function | 400 |
| $C-5$ | Shifted and Rotated Rastrigin's Function | 500 |
| $C-6$ | Shifted and Rotated Expanded Scaffer's Function | 600 |
| $C-7$ | Shifted and Rotated Lunacek Bi_Rastrigin Function | 700 |
| $C-8$ | Shifted and Rotated Non-Continuous Rastrigin's Function | 800 |
| $C-9$ | Shifted and Rotated Levy Function | 900 |
| $C-10$ | Shifted and Rotated Schwefel's Function | 1000 |
| $C-11$ | Hybrid Function 1 ($N=3$) | 1100 |
| $C-12$ | Hybrid Function 2 ($N=3$) | 1200 |
| $C-13$ | Hybrid Function 3 ($N=3$) | 1300 |
| $C-14$ | Hybrid Function 4 ($N=4$) | 1400 |
| $C-15$ | Hybrid Function 5 ($N=4$) | 1500 |
| $C-16$ | Hybrid Function 6 ($N=4$) | 1600 |
| $C-17$ | Hybrid Function 6 ($N=5$) | 1700 |
| $C-18$ | Hybrid Function 6 ($N=5$) | 1800 |
| $C-19$ | Hybrid Function 6 ($N=5$) | 1900 |
| $C-20$ | Hybrid Function 6 ($N=6$) | 2000 |
| $C-21$ | Composition Function 1 ($N=3$) | 2100 |
| $C-22$ | Composition Function 2 ($N=3$) | 2200 |
| $C-23$ | Composition Function 3 ($N=4$) | 2300 |
| $C-24$ | Composition Function 4 ($N=4$) | 2400 |
| $C-25$ | Composition Function 5 ($N=5$) | 2500 |
| $C-26$ | Composition Function 6 ($N=5$) | 2600 |
| $C-27$ | Composition Function 7 ($N=6$) | 2700 |
| $C-28$ | Composition Function 8 ($N=6$) | 2800 |
| $C-29$ | Composition Function 9 ($N=3$) | 2900 |
| $C-30$ | Composition Function 10 ($N=3$) | 3000 |

#### *A.5.8. Expanded Scaffer's $F6$ function*

Scaffer's $F6$ Function:

$$g(z,x) = 0.5 + \frac{(sin^2(\sqrt{z^2+x^2}) - 0.5)}{(1+0.001(z^2+x^2))^2}$$

$$F(z) = g(z_1,z_2) + g(z_2,z_3) + \cdots + g(z_{30},z_1)$$

#### *A.5.9. High conditioned Elliptic function*

$$F(z) = \sum_{i=1}^{30} (10^6)^{\frac{i-1}{30-1}} z_i^2$$

Note that the Weierstrass, Rosenbrock's, Griewank's, Rastrigin's, and Ackley's functions in CEC-2015 benchmark test suite are same as above mentioned $Weierstrass, F_5, F_{11}, F_9$, and $F_{10}$ benchmark test functions.

### *A.6. Composite benchmark functions*

The detailed description of six well-known composite benchmark test functions ($F_{24} - F_{29}$) are mentioned in Table A.1.

### *A.7. CEC-2015 benchmark test functions*

The detailed description of fifteen well-known CEC-2015 benchmark test functions ($CEC1 - CEC15$) are mentioned in Table A.2.

### *A.8. CEC-2017 benchmark test functions*

The detailed description of fifteen well-known CEC-2017 benchmark test functions ($C1 - C30$) are mentioned in Table A.3.

## References


Alba, E., Dorronsoro, B., 2005. The exploration/exploitation tradeoff in dynamic cellular genetic algorithms. IEEE Trans. Evol. Comput. 9 (2), 126–142.

Awad, N., Ali, M., Liang, J., Qu, B., Suganthan, P., 2016. Problem Definitions and Evaluation Criteria for the Cec 2017 Special Session and Competition on Single Objective Bound Constrained Real-Parameter Numerical Optimization. Technical Report, Nanyang Technological University Singapore.

Berrill, J., 1950. The Tuniccafa. The Royal Society, London.

Bichon, C.V.C.B.J., 2004. Design of space trusses using ant colony optimization. J. Struct. Eng. 130 (5), 741–751.

Brest, J., Maučec, M.S., Bošković, B., 2017. Single objective real-parameter optimization: algorithm jso. In: 2017 IEEE Congress on Evolutionary Computation (CEC). IEEE, pp. 1311–1318.

Chandrawat, R.K., Kumar, R., Garg, B., Dhiman, G., Kumar, S., 2017. An analysis of modeling and optimization production cost through fuzzy linear programming problem with symmetric and right angle triangular fuzzy number. In: Proceedings of Sixth International Conference on Soft Computing for Problem Solving. Springer, pp. 197–211.

Chen, Q., Liu, B., Zhang, Q., Liang, J., Suganthan, P., Qu, B., 2014. Problem Definitions and Evaluation Criteria for Cec 2015 Special Session on Bound Constrained Single-Objective Computationally Expensive Numerical Optimization. Technical Report, Computational Intelligence Laboratory, Zhengzhou University, Zhengzhou, China and Technical Report, Nanyang Technological University.

Davenport, J., Balazs, G.H., 1991. 'fiery bodies' - are pyrosomas an important component of the diet of leatherback turtles?. Br. Herpetol. Soc. Bull. 37, 33–38.

Dehghani, M., Montazeri, Z., Malik, O.P., Dhiman, G., Kumar, V., 2019. Bosa: Binary orientation search algorithm. Int. J. Innov. Technol. Explor. Eng. 9, 5306–5310.

Dhiman, G., 2019a. Esa: a hybrid bio-inspired metaheuristic optimization approach for engineering problems. Eng. Comput. 1–31.

Dhiman, G., 2019b. Multi-Objective Metaheuristic Approaches for Data Clustering in Engineering Application (S) (Ph.D. dissertation).

Dhiman, G., 2019c. Moshepo: a hybrid multi-objective approach to solve economic load dispatch and micro grid problems. Appl. Intell. 1–19.

Dhiman, G., Guo, S., Kaur, S., 2018. Ed-sho: A framework for solving nonlinear economic load power dispatch problem using spotted hyena optimizer. Modern Phys. Lett. A 33 (40).

Dhiman, G., Kaur, A., 2017. Spotted hyena optimizer for solving engineering design problems. In: 2017 International Conference on Machine Learning and Data Science (MLDS). IEEE, pp. 114–119.

Dhiman, G., Kaur, A., 2018. Optimizing the design of airfoil and optical buffer problems using spotted hyena optimizer. Designs 2 (3), 28.

Dhiman, G., Kaur, A., 2019a. A hybrid algorithm based on particle swarm and spotted hyena optimizer for global optimization. In: Soft Computing for Problem Solving. Springer, pp. 599–615.

Dhiman, G., Kaur, A., 2019b. Stoa: A bio-inspired based optimization algorithm for industrial engineering problems. Eng. Appl. Artif. Intell. 82, 148–174.

Dhiman, G., Kumar, V., 2017. Spotted hyena optimizer: A novel bio-inspired based metaheuristic technique for engineering applications. Adv. Eng. Softw. 114, 48–70.

Dhiman, G., Kumar, V., 2018a. Astrophysics inspired multi-objective approach for automatic clustering and feature selection in real-life environment. Mod. Phys. Lett. B 32 (31).

Dhiman, G., Kumar, V., 2018b. Emperor penguin optimizer: A bio-inspired algorithm for engineering problems. Knowl.-Based Syst. 159, 20–50, [Online]. Available: http://www.sciencedirect.com/science/article/pii/S095070511830296X.

Dhiman, G., Kumar, V., 2018c. Multi-objective spotted hyena optimizer: A multi-objective optimization algorithm for engineering problems. Knowl.-Based Syst. 150, 175–197.

Dhiman, G., Kumar, V., 2019a. Knrvea: A hybrid evolutionary algorithm based on knee points and reference vector adaptation strategies for many-objective optimization. Appl. Intell. 49 (7), 2434–2460.

Dhiman, G., Kumar, V., 2019b. Seagull optimization algorithm: Theory and its applications for large-scale industrial engineering problems. Knowl.-Based Syst. 165, 169–196.

Dhiman, G., Kumar, V., 2019c. Spotted hyena optimizer for solving complex and non-linear constrained engineering problems. In: Harmony Search and Nature Inspired Optimization Algorithms. Springer, pp. 857–867.

Dhiman, G., Singh, P., Kaur, H., Maini, R., 2019. Dhiman: A novel algorithm for economic d ispatch problem based on optimization met h od us i ng m onte carlo simulation and a strophysics co n cepts. Modern Phys. Lett. A 34 (04).

Digalakis, J., Margaritis, K., 2001. On benchmarking functions for genetic algorithms. Int. J. Comput. Math. 77 (4), 481–506.

Dorigo, M., Birattari, M., Stutzle, T., 2006. Ant colony optimization - artificial ants as a computational intelligence technique. IEEE Comput. Intell. Mag. 1, 28–39.

Gandomi, A.H., Yang, X.-S., 2011. Benchmark Problems in Structural Optimization. Springer Berlin Heidelberg, pp. 259–281.

Garg, M., Dhiman, G., 2020. Deep convolution neural network approach for defect inspection of textured surfaces. J. Inst. Electron. Comput. 2, 28–38.

Holland, J.H., 1992. Genetic algorithms. Sci. Amer. 267 (1), 66–72.

Kannan, B., Kramer, S.N., 1994. An augmented lagrange multiplier based method for mixed integer discrete continuous optimization and its applications to mechanical design. J. Mech. Des. 116 (2), 405–411.
Kaur, A., Dhiman, G., 2019. A review on search-based tools and techniques to identify bad code smells in object-oriented systems. In: Harmony Search and Nature Inspired Optimization Algorithms. Springer, pp. 909–921.
Kaur, A., Kaur, S., Dhiman, G., 2018. A quantum method for dynamic nonlinear programming technique using schrödinger equation and monte carlo approach. Mod. Phys. Lett. B 32 (30).
Kaveh, A., Talatahari, S., 2009a. A particle swarm ant colony optimization for truss structures with discrete variables. J. Construct. Steel Res. 65 (8–9), 1558–1568.
Kaveh, A., Talatahari, S., 2009b. Particle swarm optimizer ant colony strategy and harmony search scheme hybridized for optimization of truss structures. Comput. Struct. 87 (5–6), 267–283.
Kaveh, A., Talatahari, S., 2009c. Size optimization of space trusses using big bang-big crunch algorithm. Comput. Struct. 87 (17–18), 1129–1140, [Online]. Available: http://www.sciencedirect.com/science/article/pii/S0045794909001394.
Kaveh, A., Talatahari, S., 2010. Optimal design of skeletal structures via the charged system search algorithm. Struct. Multidiscip. Optim. 41 (6), 893–911, [Online]. Available: http://dx.doi.org/10.1007/s00158-009-0462-5.
Kennedy, J., Eberhart, R.C., 1995. Particle swarm optimization. In: Proceedings of IEEE International Conference on Neural Networks, pp. 1942–1948.
Liang, J.J., Suganthan, P.N., Deb, K., 2005. Novel composition test functions for numerical global optimization. In: Proceedings IEEE Swarm Intelligence Symposium, pp. 68–75.
Lozano, M., Garcia-Martinez, C., 2010. Hybrid metaheuristics with evolutionary algorithms specializing in intensification and diversification: Overview and progress report. Comput. Oper. Res. 37 (3), 481–497.
Mezura-Montes, E., Coello, C.A.C., 2005. Useful Infeasible Solutions in Engineering Optimization with Evolutionary Algorithms. Springer Berlin Heidelberg, pp. 652–662.
Mirjalili, S., 2016. Sca: A sine cosine algorithm for solving optimization problems. Knowl.-Based Syst. 96, 120–133, [Online]. Available: http://www.sciencedirect.com/science/article/pii/S0950705115005043.
Mirjalili, S., Mirjalili, S.M., Hatamlou, A., 2016. Multi-verse optimizer: A nature-inspired algorithm for global optimization. Neural Comput. Appl. 27 (2), 495–513, [Online]. Available: http://dx.doi.org/10.1007/s00521-015-1870-7.
Mirjalili, S., Mirjalili, S.M., Lewis, A., 2014. Grey wolf optimizer. Adv. Eng. Softw. 69, 46–61, [Online]. Available: http://www.sciencedirect.com/science/article/pii/S0965997813001853.
Rashedi, E., Nezamabadi-pour, H., Saryazdi, S., 2009. GSA: A gravitational search algorithm. Inf. Sci. 197 (31), 2232–2248, [Online]. Available: http://www.sciencedirect.com/science/article/pii/S0020025509001200.
Schutte, J., Groenwold, A., 2003. Sizing design of truss structures using particle swarms. Struct. Multidiscip. Optim. 25 (4), 261–269, [Online]. Available: http://dx.doi.org/10.1007/s00158-003-0316-5.
Singh, P., Dhiman, G., 2017. A fuzzy-lp approach in time series forecasting. In: International Conference on Pattern Recognition and Machine Intelligence. Springer, pp. 243–253.
Singh, P., Dhiman, G., 2018a. A hybrid fuzzy time series forecasting model based on granular computing and bio-inspired optimization approaches. J. Comput. Sci. 27, 370–385.
Singh, P., Dhiman, G., 2018b. Uncertainty representation using fuzzy-entropy approach: Special application in remotely sensed high-resolution satellite images (rshrsis). Appl. Soft Comput. 72, 121–139.
Singh, P., Dhiman, G., Guo, S., Maini, R., Kaur, H., Kaur, A., Kaur, H., Singh, J., Singh, N., 2019. A hybrid fuzzy quantum time series and linear programming model: Special application on taiex index dataset. Modern Phys. Lett. A 34 (25).
Singh, P., Dhiman, G., Kaur, A., 2018a. A quantum approach for time series data based on graph and schrödinger equations methods. Modern Phys. Lett. A 33 (35).
Singh, P., Rabadiya, K., Dhiman, G., 2018b. A four-way decision-making system for the indian summer monsoon rainfall. Mod. Phys. Lett. B 32 (25).
Verma, S., Kaur, S., Dhiman, G., Kaur, A., 2018. Design of a novel energy efficient routing framework for wireless nanosensor networks. In: 2018 First International Conference on Secure Cyber Computing and Communication (ICSCCC). IEEE, pp. 532–536.
Wolpert, D.H., Macready, W.G., 1997. No free lunch theorems for optimization. IEEE Trans. Evol. Comput. 1 (1), 67–82.
Yang, X.-S., 2010. Firefly algorithm stochastic test functions and design optimisation. Int. J. Bio-Inspired Comput. 2 (2), 78–84, [Online]. Available: http://dx.doi.org/10.1504/IJBIC.2010.032124.